

Patient and Specimen Information

Patient and Specimen Information	Observed Value
Accession Number	TN26-
Primary Tumor Site	Pancreas, NOS
Histology	Adenocarcinoma, NOS
Specimen Site	Liver
Dissection Type	Microdissection
Tissue Area Dissected (mm ²)	112.5

Next Generation Sequencing Metrics

Metric	Observed Value
Total DNA Reads (Million)	236.8
Mapped Reads (Million)	218.3 (92.19%)
Low Quality Reads (Million)	18.1 (7.64%)
Unmapped Reads (Million)	0.4 (0.17%)
Average Depth (WES, Targeted Panel)	321.5, 1655.8
Insert Size, Mode	145
Insert Size, 20th Percentile	129
Insert Size, 50th Percentile	166
RNA Total Reads (Million)	30.7
RNA Mapped Reads (Million)	29.0
RNA Unique Reads (Million)	25.6

TN26-

Tumor Mutational Burden (TMB) Variants

Variant	Variant	Variant
chr1: KIF1B (Y1687D)	chr6: MDN1 (D4824G)	chr14: SYT16 (D56fs)
chr1: MAD2L2 (D8N)	chr6: ROS1 ()	chr14: DIO3 (T287I)
chr1: PRAMEF1 (R375C)	chr6: SERINC1 (W178fs)	chr14: EIF5 (H305D)
chr1: PRAMEF6 (K440R)	chr6: CTAGE9 (Q9R)	chr14: AHNAK2 (R5769I)
chr1: PRAMEF6 (K440E)	chr6: NOX3 (T13N)	chr15: POTE3 (R530Q)
chr1: PRAMEF6 (A436P)	chr7: FOXK1 (Q100H)	chr15: GOLGA6C (P558T)
chr1: PRAMEF6 (I434L)	chr7: AUTS2 (H633_L635del)	chr16: RAB11FIP3 (S761T)
chr1: PRAMEF6 (Y413H)	chr7: SEMA3E (L644S)	chr16: SLX4 (L530V)
chr1: PRAMEF6 (L408I)	chr7: MUC12 (E3406K)	chr16: ADCY9 (N693I)
chr1: PRAMEF6 (K406N)	chr7: CUX1 (A1406fs)	chr16: ZNF771 (G50A)
chr1: PRAMEF6 (I404R)	chr7: CNOT4 (N345S)	chr16: SALL1 (G967A)
chr1: PRAMEF27 (D245E)	chr7: PRSS2 (I102F)	chr16: NPIP815 (E206Q)
chr1: PRAMEF33 (D469H)	chr7: ACTR3C (W123S)	chr17: PFAS (E37Q)
chr1: PRAMEF14 (M28V)	chr7: CRYGN (N127K)	chr17: KLHL11 (S346C)
chr1: PRAMEF14 (S24A)	chr7: ACTR3B (W252S)	chr17: TAC4 (Q51L)
chr1: PRAMEF14 (G14V)	chr8: PRAG1 (S574N)	chr17: CEP112 (K412I)
chr1: UBR4 (V1644F)	chr8: LOXL2 (A539fs)	chr17: QRICH2 (A615G)
chr1: DENND2C (F394L)	chr8: RBPMS (R45T)	chr17: QRICH2 (A611V)
chr1: NBPF15 (R121H)	chr8: GTF2E2 (H273D)	chr18: L3MBTL4 (A497E)
chr1: RPTN (G104R)	chr8: ADGRA2 (V516L)	chr18: APCDD1 (S32C)
chr1: EFNA1 (L187H)	chr8: PTDSS1 (K472N)	chr18: LAMA3 (A3098T)
chr1: FMO1 (I22V)	chr8: PHF20L1 (W97C)	chr18: CABYR (S201R)
chr1: CCDC185 (F583L)	chr8: EPPK1 (V2860M)	chr18: TAF4B (N336H)
chr1: LEFTY1 (A247S)	chr8: CPSF1 (L50_N53del)	chr18: ELOA3B (K260R)
chr1: TAF5L (G424E)	chr9: SPATA31A6 (P199T)	chr18: KATNAL2 (A534D)
chr1: COG2 (D519N)	chr9: SPATA31A6 (S1089I)	chr19: GRIN3B (A122G)
chr1: MAP10 (G227fs)	chr9: TGFBR1 (A24fs)	chr19: IL27RA (L445F)
chr1: LYST (Q771_D772insIM)	chr9: FRRS1L (G90fs)	chr19: WIZ (E190Q)
chr1: LYST (Q771L)	chr9: FRRS1L (G90C)	chr19: RBM42 (G219V)
chr2: WDR35 (A819S)	chr9: CEL (A626P)	chr19: ZFP82 (I495T)

TN26-

Variant	Variant	Variant
chr2: C2orf71 (A374T)	chr9: CEL (P638A)	chr19: WDR87 (L800F)
chr2: CEBPZ (L61S)	chr10: ARHGAP21 (L729F)	chr19: ZNF473 (K560M)
chr2: SPRED2 (R200T)	chr10: DLG5 (T1324I)	chr19: SHANK1 (G2074E)
chr2: SH3RF3 (L243V)	chr10: MMRN2 (T512K)	chr19: CEACAM18 (I206L)
chr2: MOGAT1 (F129L)	chr10: MMS19 (A10fs)	chr19: ZNF787 (C96R)
chr2: SNED1 (E851*)	chr10: ATRNL1 (Q934K)	chr19: ZNF460 (I555fs)
chr2: HDLBP (E1107*)	chr11: MUC5AC (P1558L)	chr19: ZNF460 (I555R)
chr3: CTNNB1 (L156P)	chr11: MUC5AC (G3185R)	chr19: ZNF460 (E557fs)
chr3: USF3 (H1437P)	chr11: OR52B2 (L261S)	chr19: ZNF460 (E558delinsDPR)
chr3: MAATS1 (S615C)	chr11: INSC (E338*)	chr19: ZNF460 (T559I)
chr3: COL6A5 (Y28fs)	chr11: MRPL16 (S135T)	chr20: RSP04 (Q65*)
chr3: PRR23A (E224K)	chr11: CASP1 (L30S)	chr20: ITPA (R179G)
chr3: GMNC (L212P)	chr11: NLRX1 (E447D)	chr20: SLC23A2 (A73S)
chr4: MAN2B2 (G904V)	chr11: OR10G4 (V214L)	chr20: RIN2 (I163fs)
chr4: SLC4A4 (H369R)	chr11: ROBO3 (A1012T)	chr20: CPNE1 (F63L)
chr4: PRSS48 (Q44R)	chr12: PHC1 (M1001I)	chr21: C21orf2 (G101D)
chr5: PAPD7 (S129W)	chr12: KRT78 (I410F)	chr21: KRTAP10-9 (C251S)
chr5: LMBRD2 (L330P)	chr12: GRIP1 (D374G)	chr21: PCNT (A880S)
chr5: BDP1 (K941E)	chr12: RFX4 (M710I)	chr22: PRAME (S142G)
chr5: ADGRV1 (A2473S)	chr12: FOXP4 (I426M)	chr22: NIPSNAP1 (S281P)
chr5: FBN2 (T1758I)	chr12: FOXP4 (R311_T312insAH)	chr22: MTMR3 (V1225A)
chr5: PCDHGA7 (A706P)	chr13: PARP4 (I675M)	chrX: IGBP1 (E207D)
chr6: GMDS (L120I)	chr13: IRS2 (P588A)	chrX: SPANXB1 (Q42P)
chr6: MDC1 (S1225Y)	chr14: MYH6 (E1041_Q1042insKK)	chrX: FLNA (D1692H)
chr6: COL12A1 (E1611Q)	chr14: MYH6 (L1040Q)	

Tumor Mutational Burden by Whole Exome Sequencing (WES) Methods:

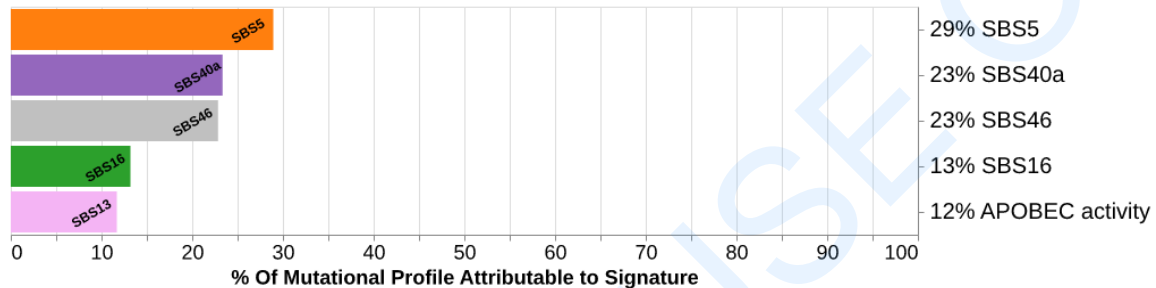
Samples with a depth of coverage on reportable genes (720 genes) lower than 100x are considered indeterminate. On samples with sufficient coverage, variants with at least 5% allele frequency identified across the whole exome are filtered to remove low quality, low depth, non-coding, synonymous, and other types that have been determined to be unreliable or unassociated with TMB. Any presumed germline variants which belong to gnomAD (AC>0), dbSNP 151 common or were found in at least 10% of training samples are also excluded. From the filtered list, missense, nonsense, in-frame INDEL, and frameshift variants in selected coding regions (25.5 Mb) with sufficient depth in training samples are counted. The final value is the variant count (displayed in the table above) divided by the length of the selected coding regions, presented as mutations/Mb. We consider samples containing 10 per Mb to be TMB high.

TN26-

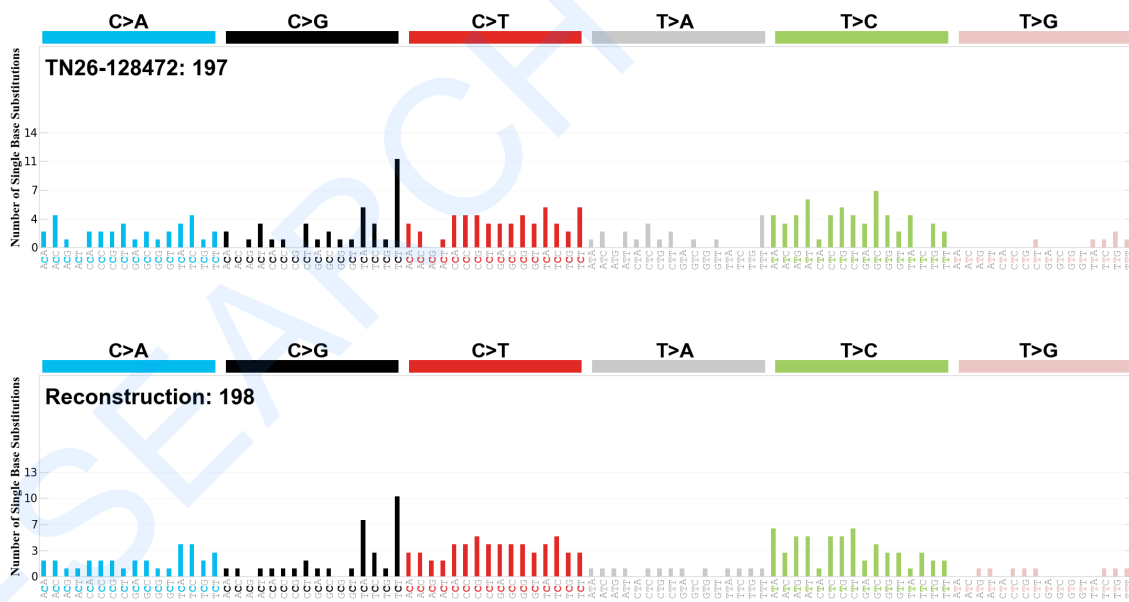
COSMIC Signatures

Metric	Result
TMB	6 per Mb
SBS Count	197
Reconstruction Accuracy	0.809

Signature Decomposition



Signature Reconstruction



COSMIC Methods:

Single base substitutions detected by Whole Exome Sequencing were used to evaluate similarity between the patient's mutation profile and established molecular phenotypes.

Alexandrov LB, Kim J, Haradhvala NJ, et al. The repertoire of mutational signatures in human cancer. Nature 578, 94-101 (2020).

TN26-

HRD - Genomic Scar Score

Component	Score
gLOH	14
LST	18
HRD-GSS	32

HRD-Genomic Scar Score (HRD-GSS) methods:

A measure of accumulated genomic instability in cells and is calculated by combining the total levels of genome-wide loss of heterozygosity (LOH) and large-scale chromosomal transitions (LST). To calculate LOH, the 22 autosomal chromosomes are split into 552 segments and the LOH of single nucleotide polymorphisms (SNPs) within each segment is calculated. Caris data consist of approximately 250k SNPs spread across the genome. SNP alleles with frequencies skewed towards 0 or 100% indicate LOH (heterozygous SNP alleles have a frequency of 50%). LST are detected when chromosomal breakages generate chromosomal gains or losses of 10 Mb or greater.

NOTE: The threshold for a high HRD-GSS (gLOH+LST) was determined and validated in a cohort consisting only of ovarian cancer patients. Caris' HRD-GSS cutoff for ovarian cancer is HRD-GSS \geq 46, with an inconclusive range of 38-45. The clinical significance of this HRD-GSS measurement outside of ovarian cancer has not been established.

Pathogen Identification

Pathogen	Reads	Threshold	Result
EBV	0	100,000	Negative
HPV16	0	300	Negative
HPV18	0	300	Negative
HPV31	0	300	Negative
HPV33	0	300	Negative
HPV34	0	---	---
HPV39	0	---	---
HPV45	0	300	Negative
HPV51	0	---	---
HPV52	0	---	---
HPV56	0	---	---
HPV58	0	---	---
HPV59	0	---	---
HPV66	0	---	---
HPV70	0	---	---
KSHV (HHV-8)	0	---	---
MCPyV	12	1,000	Negative

--- Denotes that the value is not clinically reportable and does not have an associated qualitative value or threshold.

Epstein-Barr virus (EBV) detection by Whole Exome Sequencing (WES) Methods:

The DNA of EBV must be detected for a tumor to be considered positive for EBV. This EBV-detection assay determines EBV-status using WES to enumerate the number of sequencing reads specific to EBV. EBV is commonly found in gastric/esophageal junction carcinomas (EJC) and nasopharyngeal carcinoma (NPC) of the head and neck. EBV-positive gastric/EJC and NPC tumors exhibit molecular hallmarks of potential sensitivity to cancer immunotherapy: EBV-positivity has been associated with partial responses to immunotherapy in gastric/EJC cancer, and define an undifferentiated subtype with superior prognosis and an immune-dense microenvironment in NPC.

Human papilloma virus (HPV) 16/18/31/33/45-detection by Whole Exome Sequencing (WES) Methods:

The DNA of HPV types 16, 18, 31, 33 or 45 must be detected for a tumor to be considered positive for HPV. This HPV-detection assay determines HPV-status using WES to enumerate the number of sequencing reads specific to aforementioned HPV types. HPV 16, 18, 31, 33 and 45 are among the most prevalent HPV genotypes associated with oral and anogenital cancers (including cervical, vulvar, anal, penile and oropharyngeal). Generally, HPV-associated etiology has been associated with improved prognosis, de-intensified treatment protocols and tumor subclassification. Tumors commonly ascribed to HPV etiology are most common in squamous cell carcinomas including cervical, vulvar, anal, penile and oropharyngeal. If positive, HPV has been associated with improved prognosis, de-intensified treatment protocols and tumor subclassification. Other HPV subtypes may not have sufficient coverage to be reliably detected and therefore should not be considered negative results.

Merkel Cell Polyomavirus (MCPyV) detection by Whole Exome Sequencing (WES) Methods:

This MCPyV detection assay determines MCPyV status using WES to enumerate the number of sequencing reads specific to MCPyV. MCPyV positivity is associated with the pathogenesis of Merkel Cell Carcinoma (MCC). MCC tumors that are MCPyV-positive typically have more stable genomes and lower mutational burden than those that are MCPyV-negative.

Kaposi sarcoma-associated herpesvirus (KSHV, HHV-8) detection by Whole Exome Sequencing (WES) Methods:

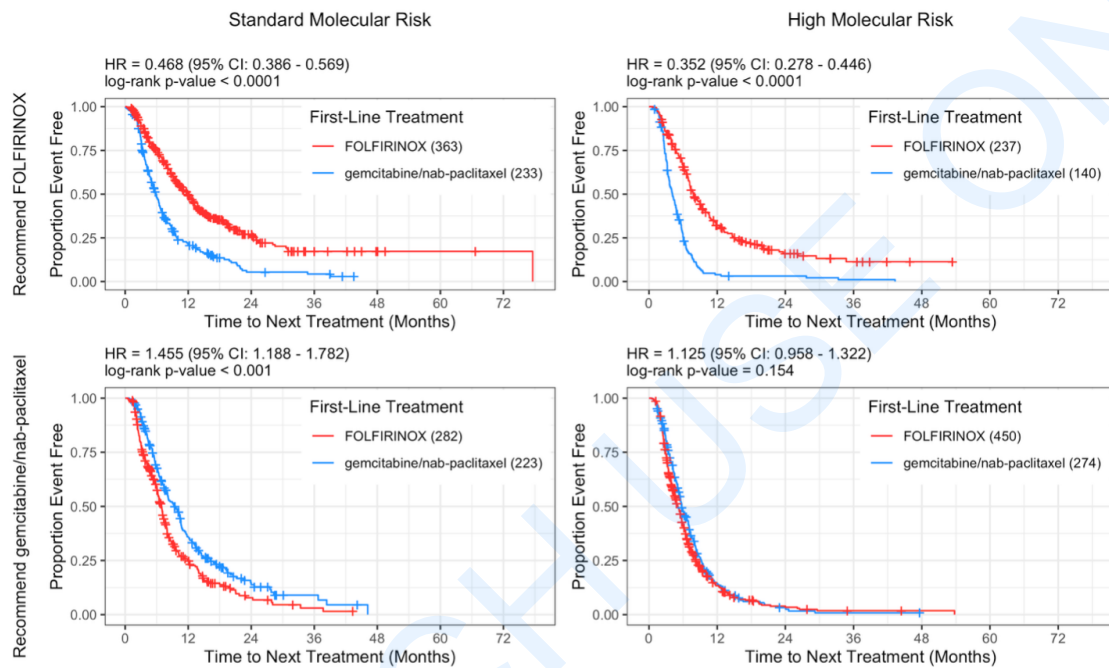
Kaposi sarcoma-associated herpesvirus (KSHV), also known as Human Herpesvirus-8 (HHV-8) is commonly found in Kaposi sarcoma tumors.

TN26-

Caris AI Insights™

PANcAI: First-line Treatment Predictor for Late Stage Pancreatic Adenocarcinoma

Recommended Therapy	Molecular Risk (High/Standard)
Gemcitabine/Nab-Paclitaxel	Standard



Pancreatic Adenocarcinoma Treatment Predictor Methods:

The Pancreatic AI Insight™ uses paired Whole Exome Sequencing (WES) and Whole Transcriptome Sequencing (WTS) to support first-line regimen selection in advanced/metastatic pancreatic ductal adenocarcinoma (PDAC) between FOLFIRINOX and gemcitabine plus nab-paclitaxel (gem/nab-p). The product reports (1) a treatment recommendation (FOLFIRINOX vs gem/nab-p) and (2) a molecular risk designation (standard vs high) to provide prognostic context within the recommended regimen. The model was developed using 2,202 molecularly profiled PDAC cases with claims-linked real-world outcomes (FOLFIRINOX n = 1,332; gem/nab-p n = 870). The training endpoint was time to next treatment (TTNT) measured from initiation of first-line therapy, used as a real-world proxy for durability of benefit and was not informed by overall survival or subsequent treatment decisions. Candidate inputs included WTS-derived expression features and DNA-derived features along with established PDAC biology signals, including the PurIST subtype. Patients recommended for FOLFIRINOX by the model demonstrated substantially better TTNT outcomes when they received FOLFIRINOX compared with gem/nab-p. Within the standard molecular risk subgroup, patients recommended to receive FOLFIRINOX and received the regimen demonstrated a median TTNT of 11.9 months compared to 5.9 months for those treated with gem/nab-p (Cox HR = 0.425; p < 0.0001). Patients recommended for gem/nab-p generally showed comparable TTNT outcomes across molecular risk, supporting the clinical interpretation that some patients may be reasonable candidates for treatment de-escalation to gem/nab-p without compromising durability of benefit. This Caris AI Insight™ is intended as a decision-support tool to complement standard clinical considerations (performance status, comorbidities, symptom burden, and patient goals) when selecting between two accepted first-line PDAC regimens. TTNT can be influenced by factors beyond disease progression (e.g., tolerability, access, physician practice patterns, and patient preference), so results should be interpreted in the full clinical context. Kaplan-Meier curves for TTNT are provided for the appropriate recommendation/risk group to support interpretation of the reported result in the study context.

Pancreatic Cancer Classification

Signature	Result
purIST	Strong Classical

purIST methods:

Reference: Singh H, Xiu J, Kapner KS, Yuan C, Narayan RR, Oberley M, Farrell A, Surana R, Huffman BM, Perez K, Cleary JM, Jordan AC, Dias Costa A, Williams HL, Raghavan S, Weinberg B, Pishvaian MJ, Shroff RT, Goel S, Dougan SK, Nowak JA, Spetzler D, Sledge G, Wolpin BM, Aguirre AJ. Clinical and Genomic Features of Classical and Basal Transcriptional Subtypes in Pancreatic Cancer. Clin Cancer Res. 2024 Nov 1;30(21):4932-4942. doi: 10.1158/1078-0432.CCR-24-1164. PMID: 39283131.

Six molecular subtypes of pancreatic adenocarcinoma are defined below.

purIST Subtypes

- (1) Strong Classical - Gene expression profile shows pronounced classical traits, overall best prognosis and treatment responsiveness.
- (2) Likely Classical - Gene expression profile shows moderate level of classical traits.
- (3) Lean Classical - Gene expression profile shows some level of classical traits.
- (4) Lean Basal-like - Gene expression profile shows some level of basal markers.
- (5) Likely Basal-like - Gene expression profile shows moderate level of basal markers.
- (6) Strong Basal-like - Gene expression profile shows strongly expressed basal markers, overall associated with poorest prognosis and treatment responsiveness.

TN26-

Tumor Infiltrating Immune Cells

Cell Type	QuantiSeq Fraction	Epic Fraction	MCP Counter Percentile
B cell	0.066	0.001	20
Cancer associated fibroblast	-	0.114	57
Cytotoxicity score	-	-	12
Endothelial cell	-	0.036	47
Macrophage	-	0.011	-
Macrophage M1	0.023	-	-
Macrophage M2	0.036	-	-
Monocyte	0.000	-	50
Myeloid dendritic cell	0.010	-	38
NK cell	0.045	0.000	70
Neutrophil	0.034	-	14
T cell	-	-	35
T cell CD4+	-	0.027	-
T cell CD4+ (non-regulatory)	0.075	-	-
T cell CD8+	0.000	0.024	35
T cell regulatory (Tregs)	0.008	-	-
Uncharacterized cell	0.703	0.786	-

Tumor Infiltrating Lymphocytes methods:

Tumor Infiltrating Lymphocytes in the immune microenvironment is a gene expression-based calculation for quantitating the immune context in tumor cells. By counting the expression of certain immune cell markers and expression profiles, a fraction of infiltrating immune cells can be estimated. quanTIseq methodology is utilized for the calculation.

Reference: Finotello F, Mayer C, Plattner C, et al. Molecular and pharmacological modulators of the tumor immune contexture revealed by deconvolution of RNA-seq data Genome Med. 2019 Jul 29;11(1):50.

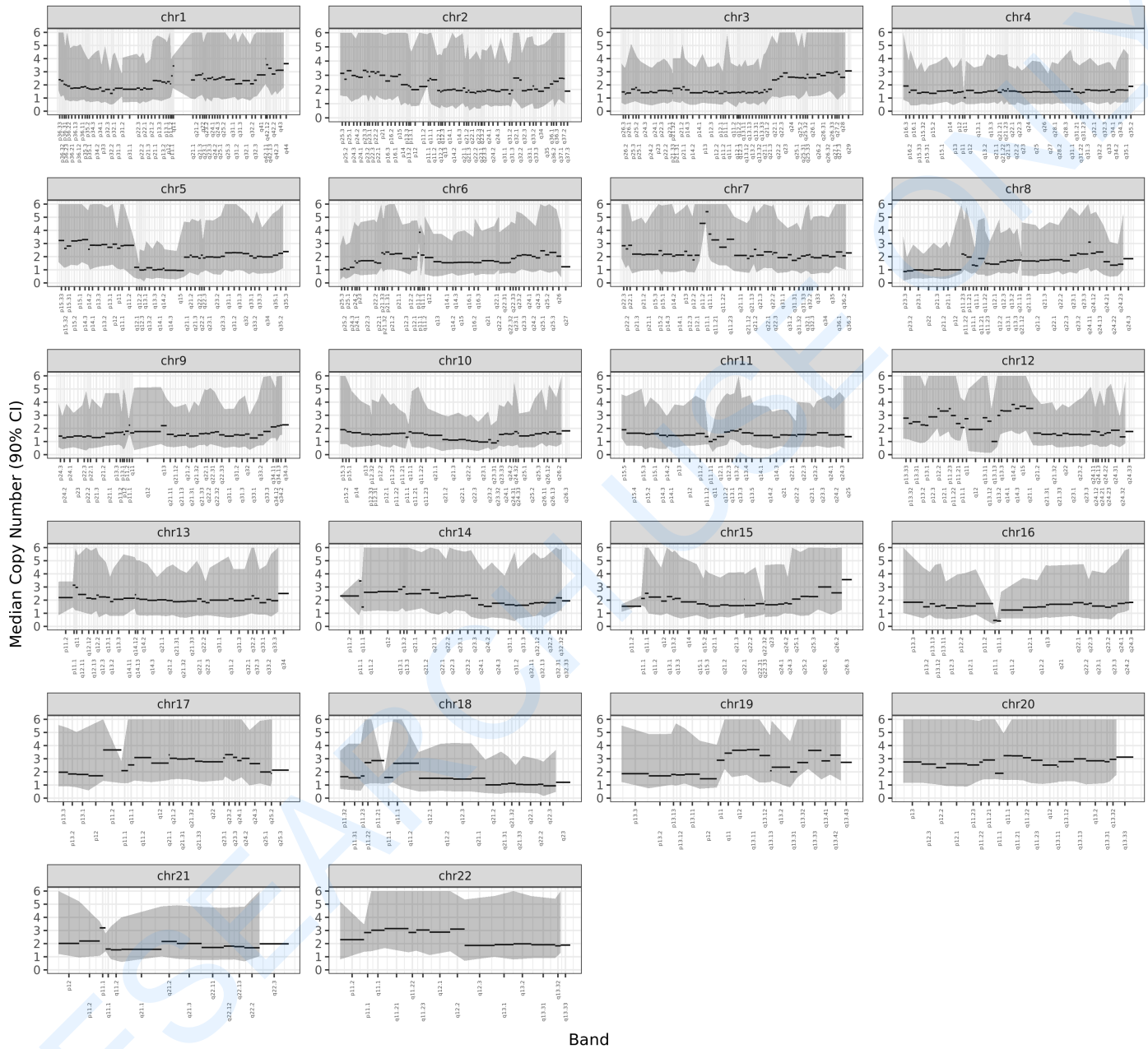
Reference: Racle J, de Jonge K, Baumgaertner P, et al. Simultaneous enumeration of cancer and immune cell types from bulk tumor gene expression data. ELife 2017.

Reference: Becht E, Giraldo N, Lacroix L, et al. Estimating the population abundance of tissue-infiltrating immune and stromal cell populations using gene expression. Genome Bio. 2016 Oct 20;17(1):218.

TN26-



Band-Level Karyotype



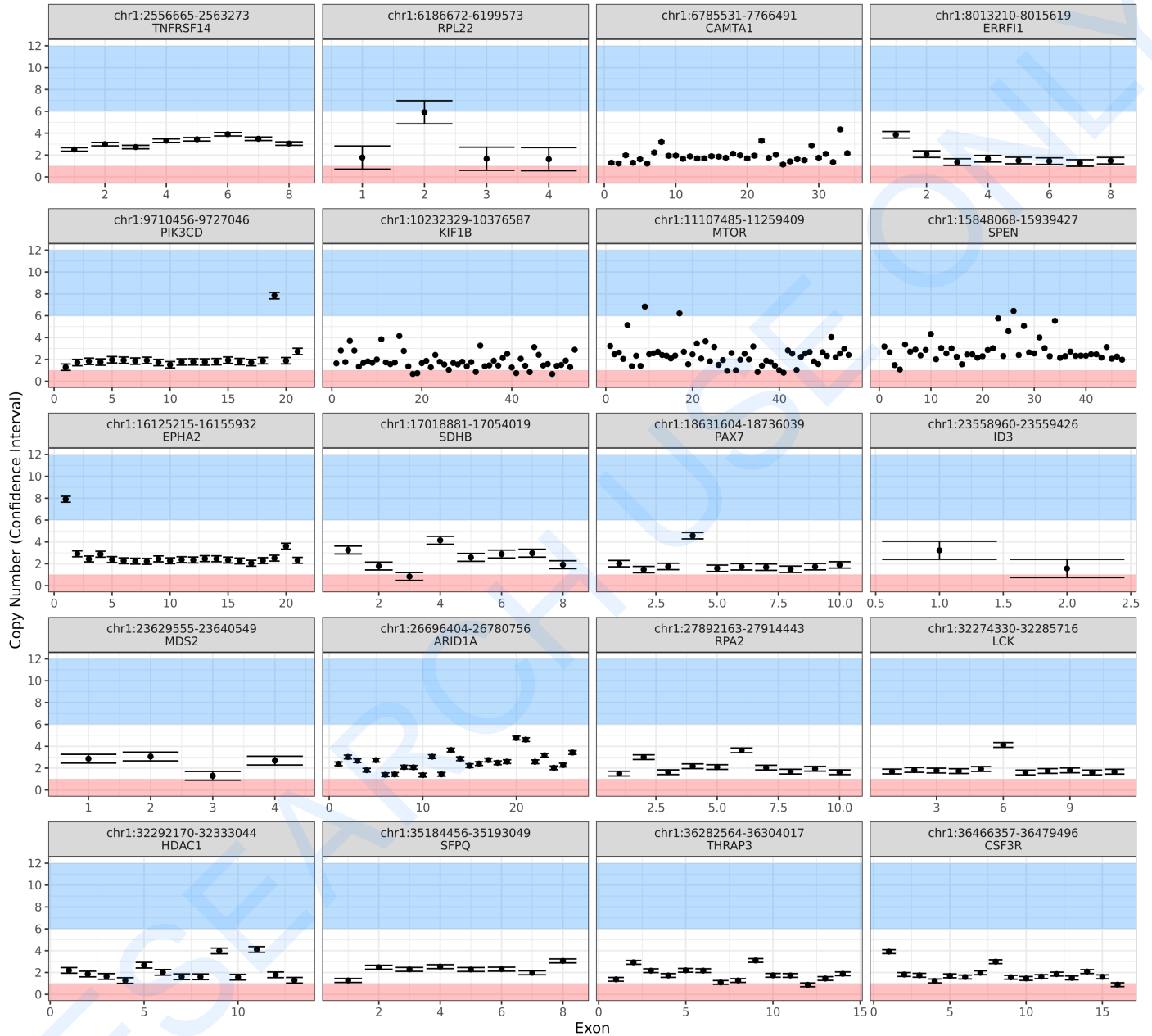
Karyotyping using Copy Number Analysis by Whole Exome Sequencing (WES) Methods:

Band-level karyotyping is the process of analyzing chromosomes to identify structure, number and potential abnormalities via cytogenetic staining techniques. Band-level analysis was performed here to estimate copy number across the karyotype: y-axis - median copy number (90% confidence interval range) along the length of each chromosome (x-axis).

TN26-



Copy Number Alterations

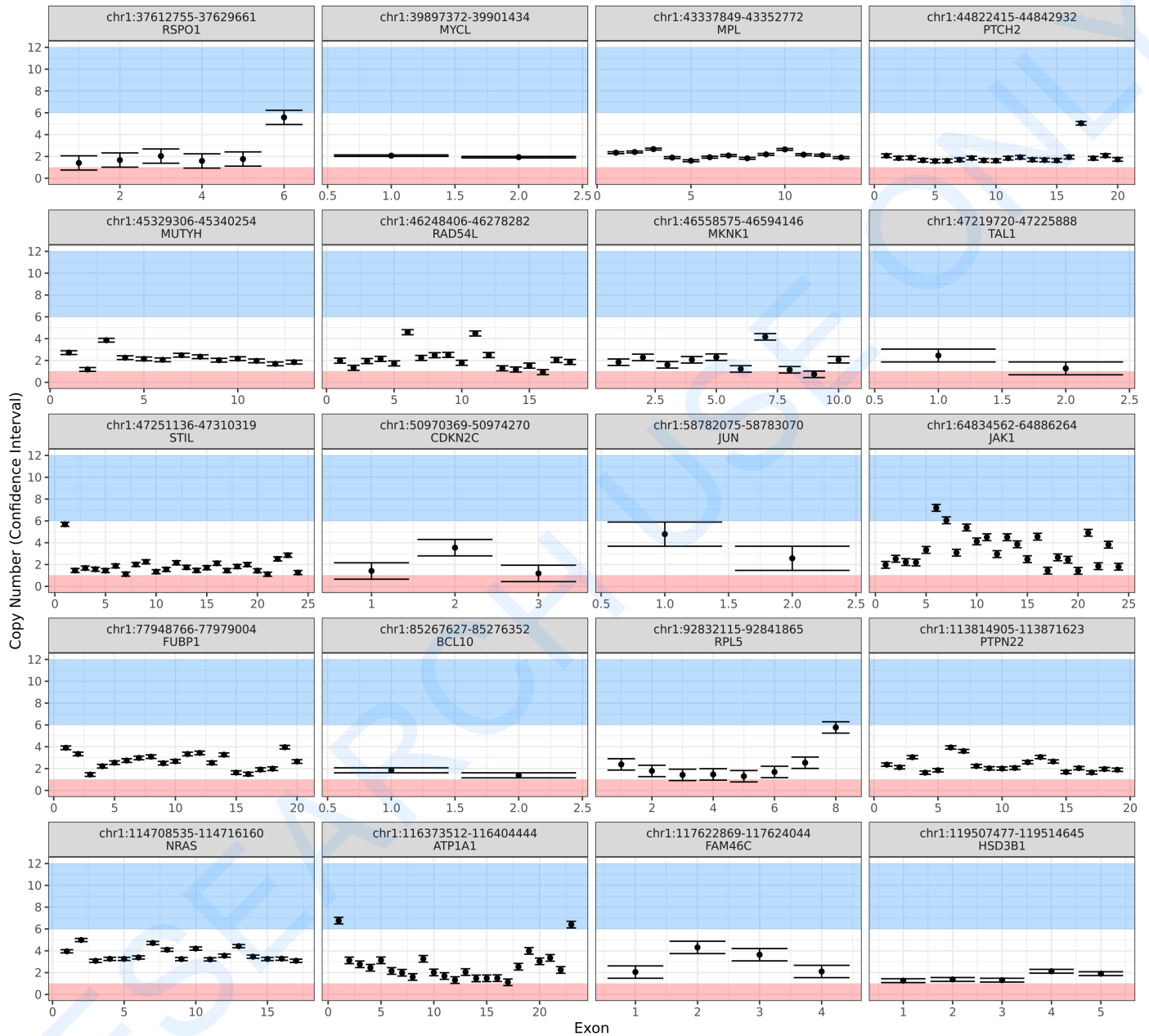


Copy number alterations by whole exome sequencing (WES):

The following plots provide estimated copy number values (black circle, y-axis) of exons per gene (x-axis), organized by chromosome (grey headers). Respective confidence intervals of each copy number call is also plotted for examining statistical error associated with next generation sequencing. Values are currently capped at 12 copies.



Copy Number Alterations

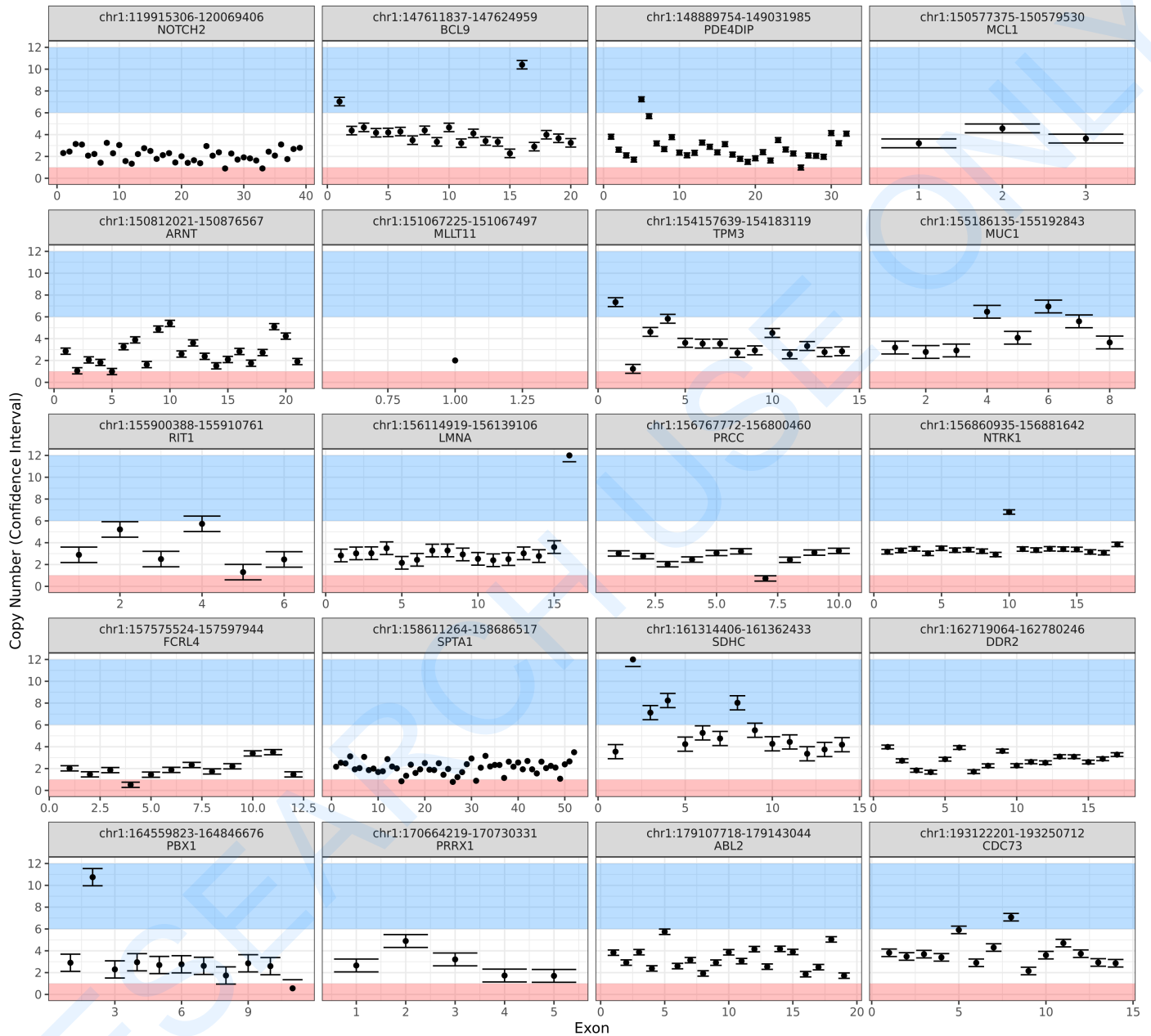


Copy number alterations by whole exome sequencing (WES):

The following plots provide estimated copy number values (black circle, y-axis) of exons per gene (x-axis), organized by chromosome (grey headers). Respective confidence intervals of each copy number call is also plotted for examining statistical error associated with next generation sequencing. Values are currently capped at 12 copies.



Copy Number Alterations

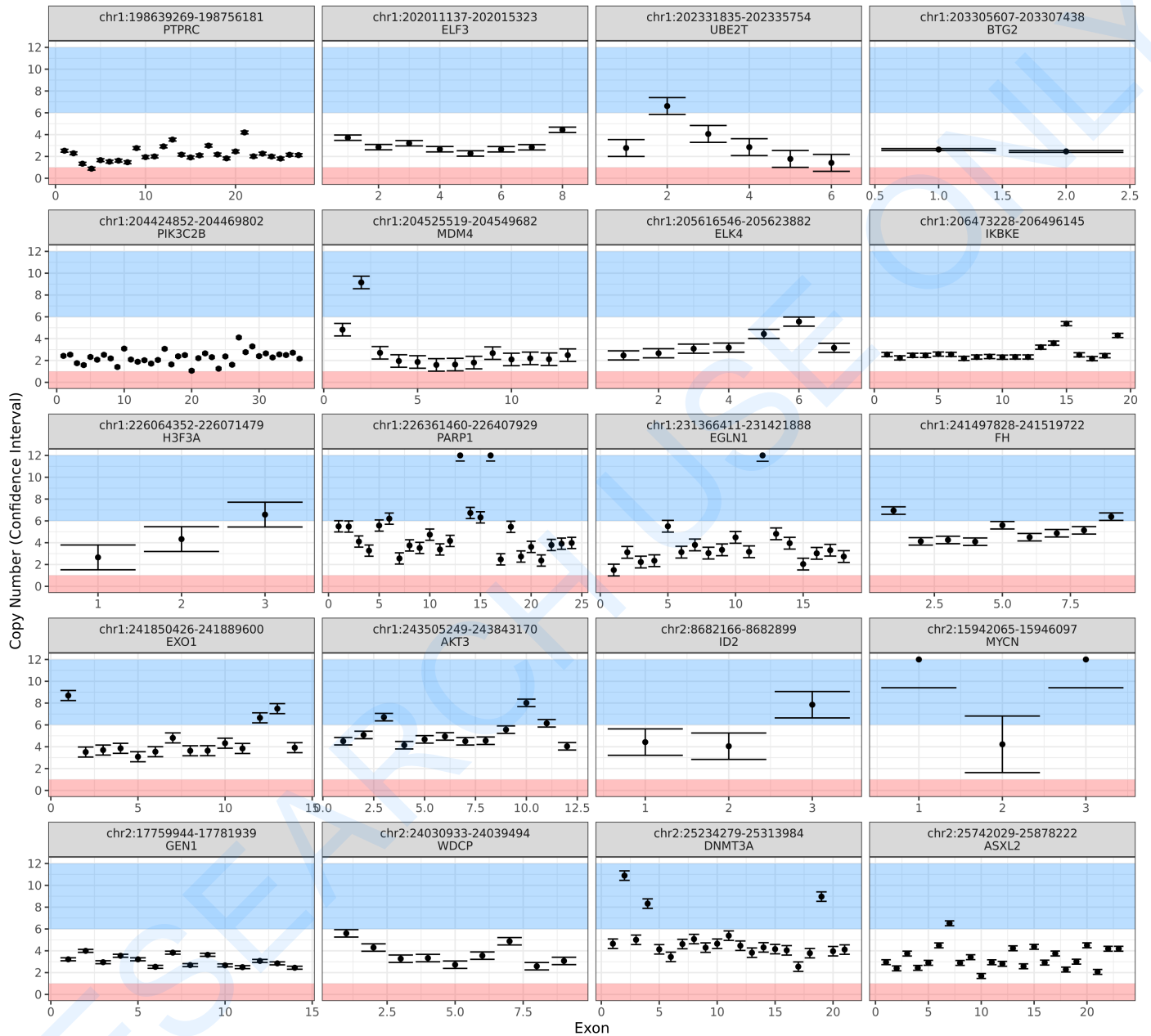


Copy number alterations by whole exome sequencing (WES):

The following plots provide estimated copy number values (black circle, y-axis) of exons per gene (x-axis), organized by chromosome (grey headers). Respective confidence intervals of each copy number call is also plotted for examining statistical error associated with next generation sequencing. Values are currently capped at 12 copies.



Copy Number Alterations

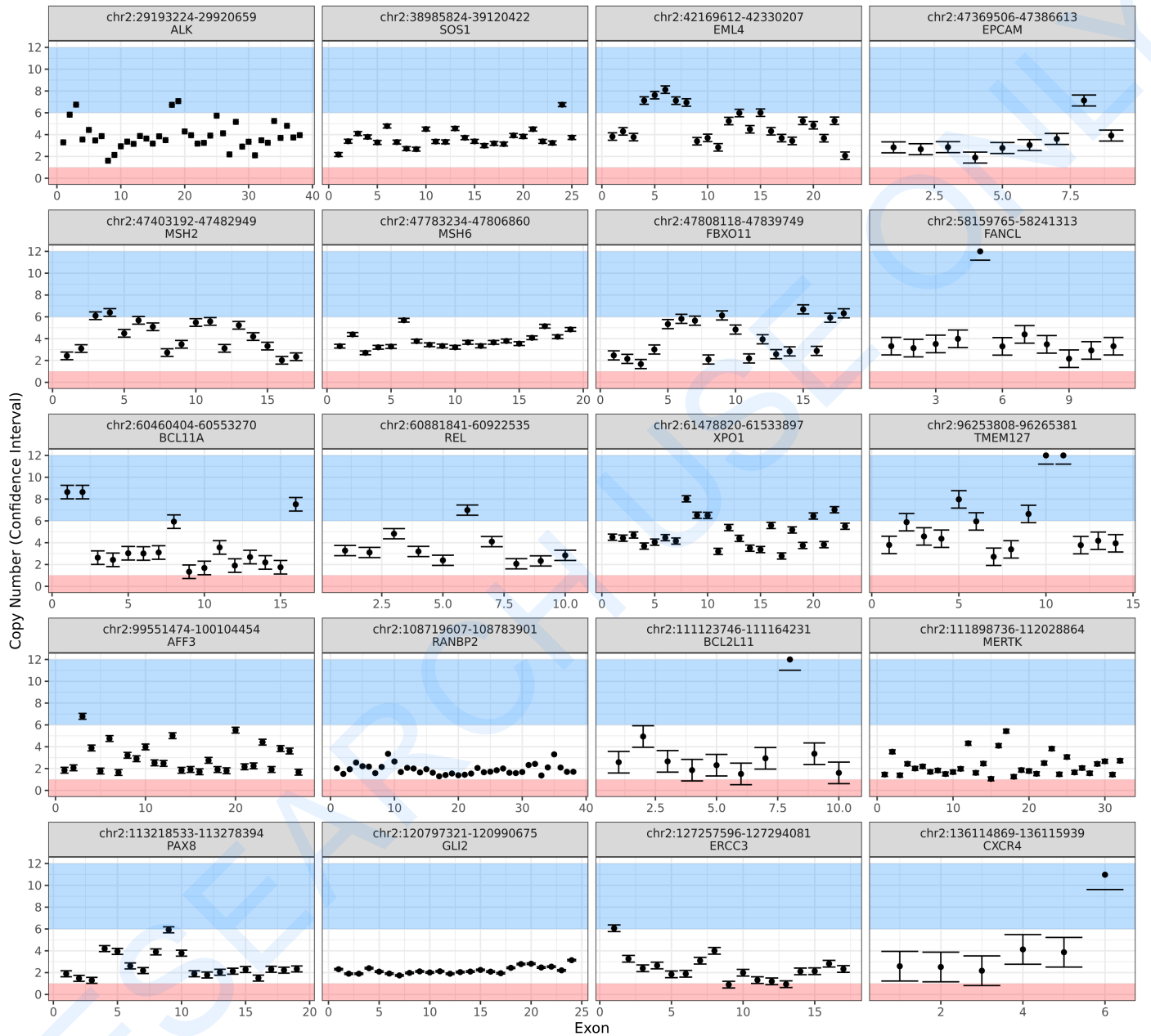


Copy number alterations by whole exome sequencing (WES):

The following plots provide estimated copy number values (black circle, y-axis) of exons per gene (x-axis), organized by chromosome (grey headers). Respective confidence intervals of each copy number call is also plotted for examining statistical error associated with next generation sequencing. Values are currently capped at 12 copies.



Copy Number Alterations

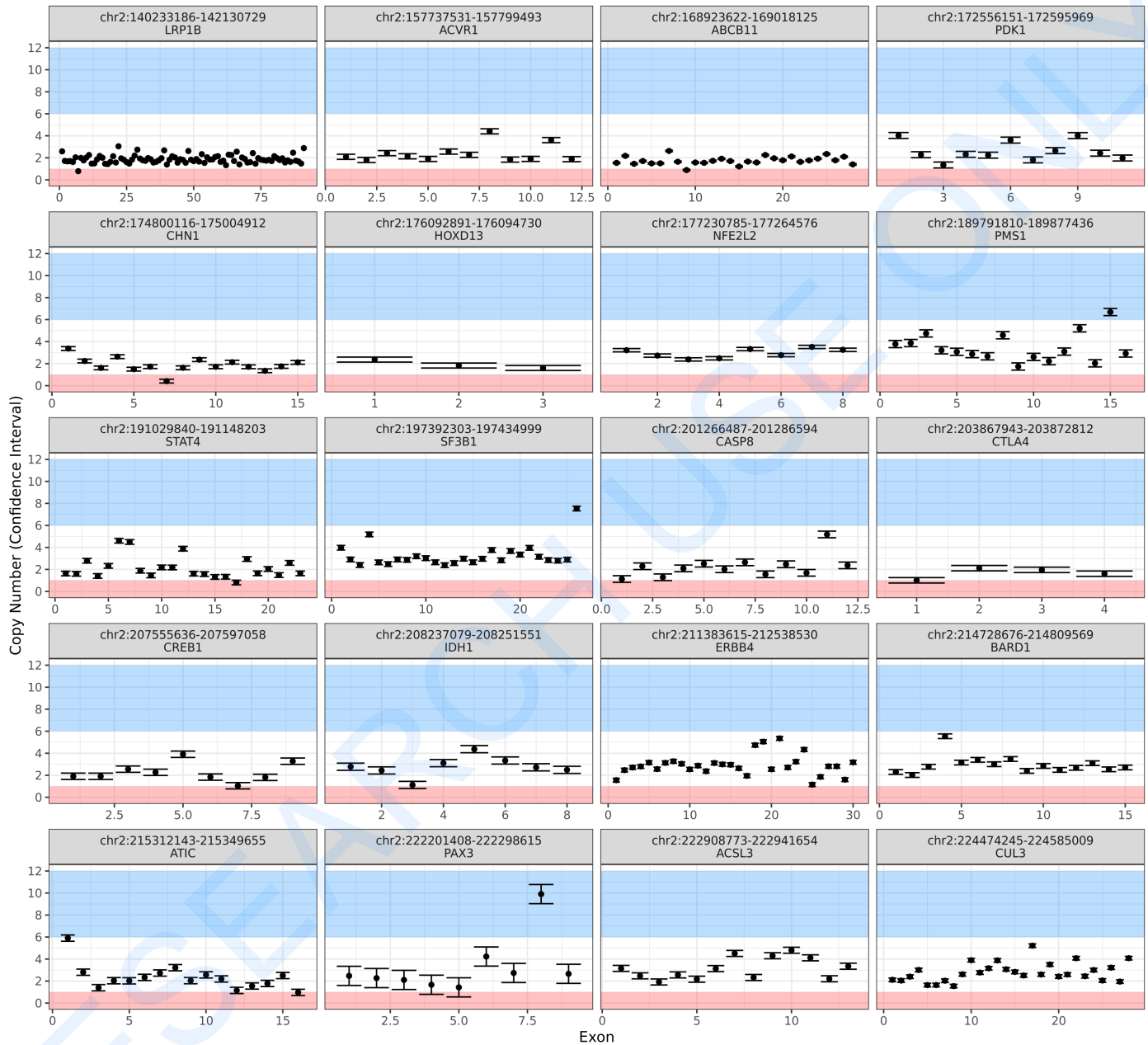


Copy number alterations by whole exome sequencing (WES):

The following plots provide estimated copy number values (black circle, y-axis) of exons per gene (x-axis), organized by chromosome (grey headers). Respective confidence intervals of each copy number call is also plotted for examining statistical error associated with next generation sequencing. Values are currently capped at 12 copies.



Copy Number Alterations

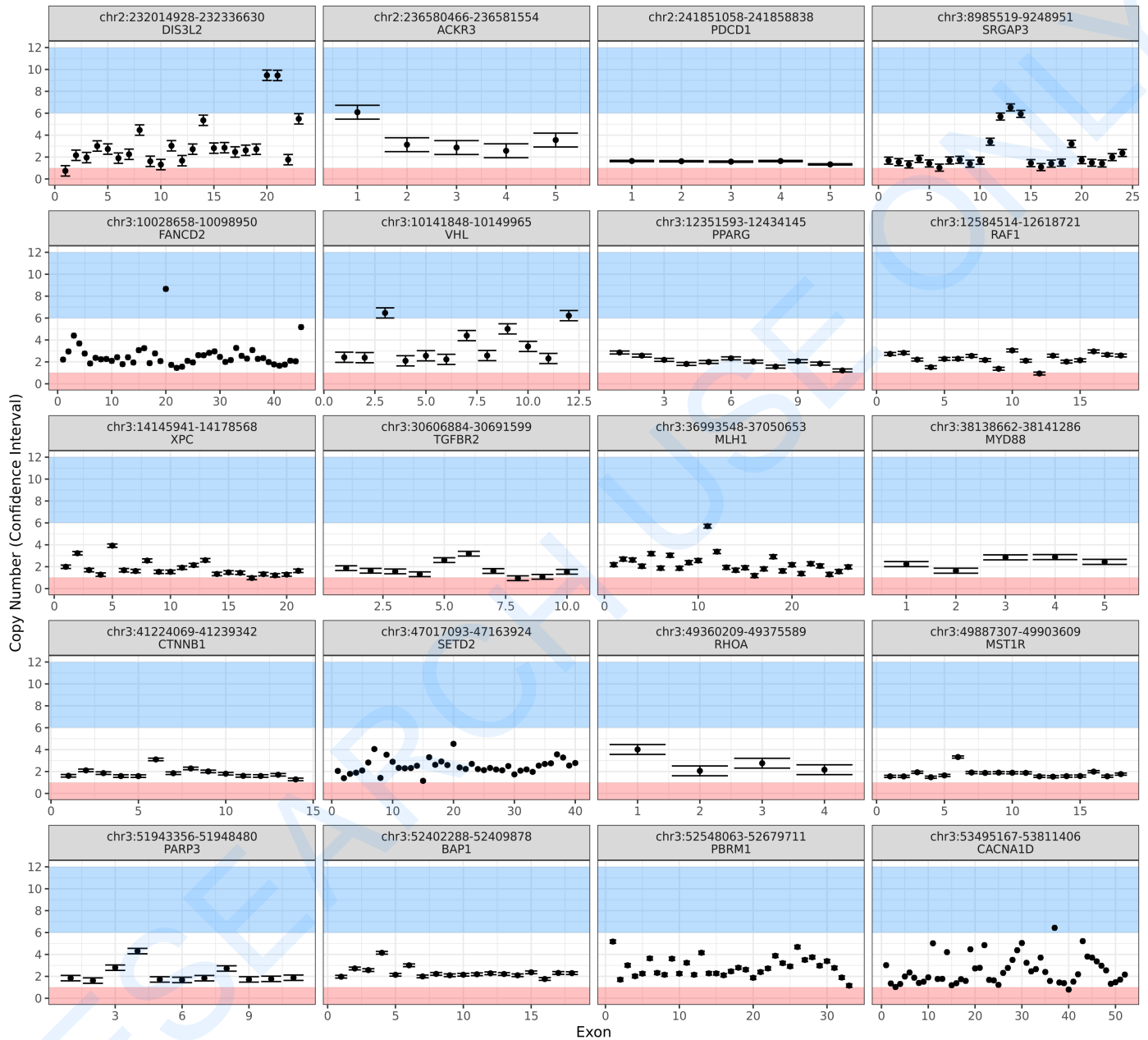


Copy number alterations by whole exome sequencing (WES):

The following plots provide estimated copy number values (black circle, y-axis) of exons per gene (x-axis), organized by chromosome (grey headers). Respective confidence intervals of each copy number call is also plotted for examining statistical error associated with next generation sequencing. Values are currently capped at 12 copies.



Copy Number Alterations

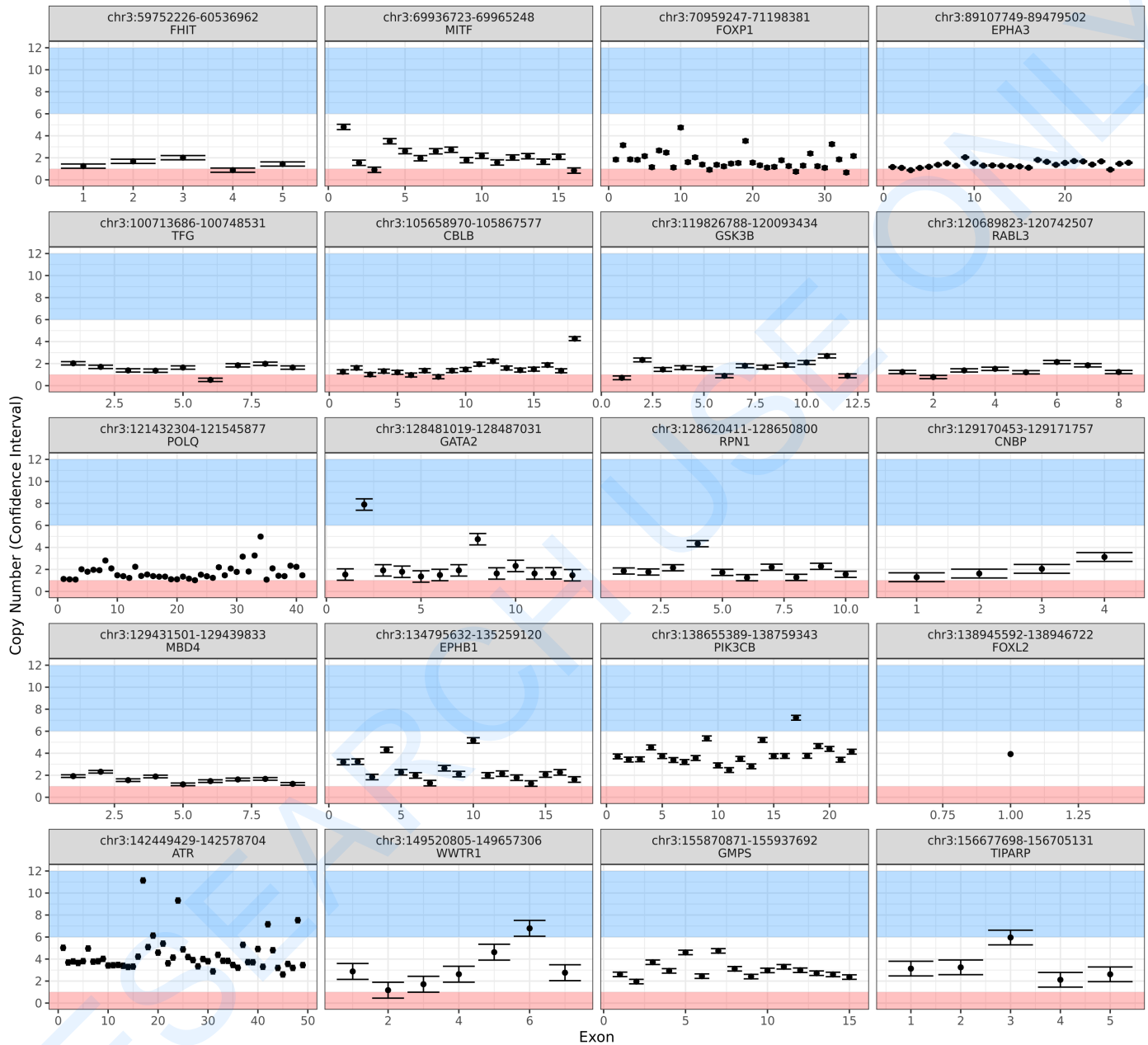


Copy number alterations by whole exome sequencing (WES):

The following plots provide estimated copy number values (black circle, y-axis) of exons per gene (x-axis), organized by chromosome (grey headers). Respective confidence intervals of each copy number call is also plotted for examining statistical error associated with next generation sequencing. Values are currently capped at 12 copies.



Copy Number Alterations

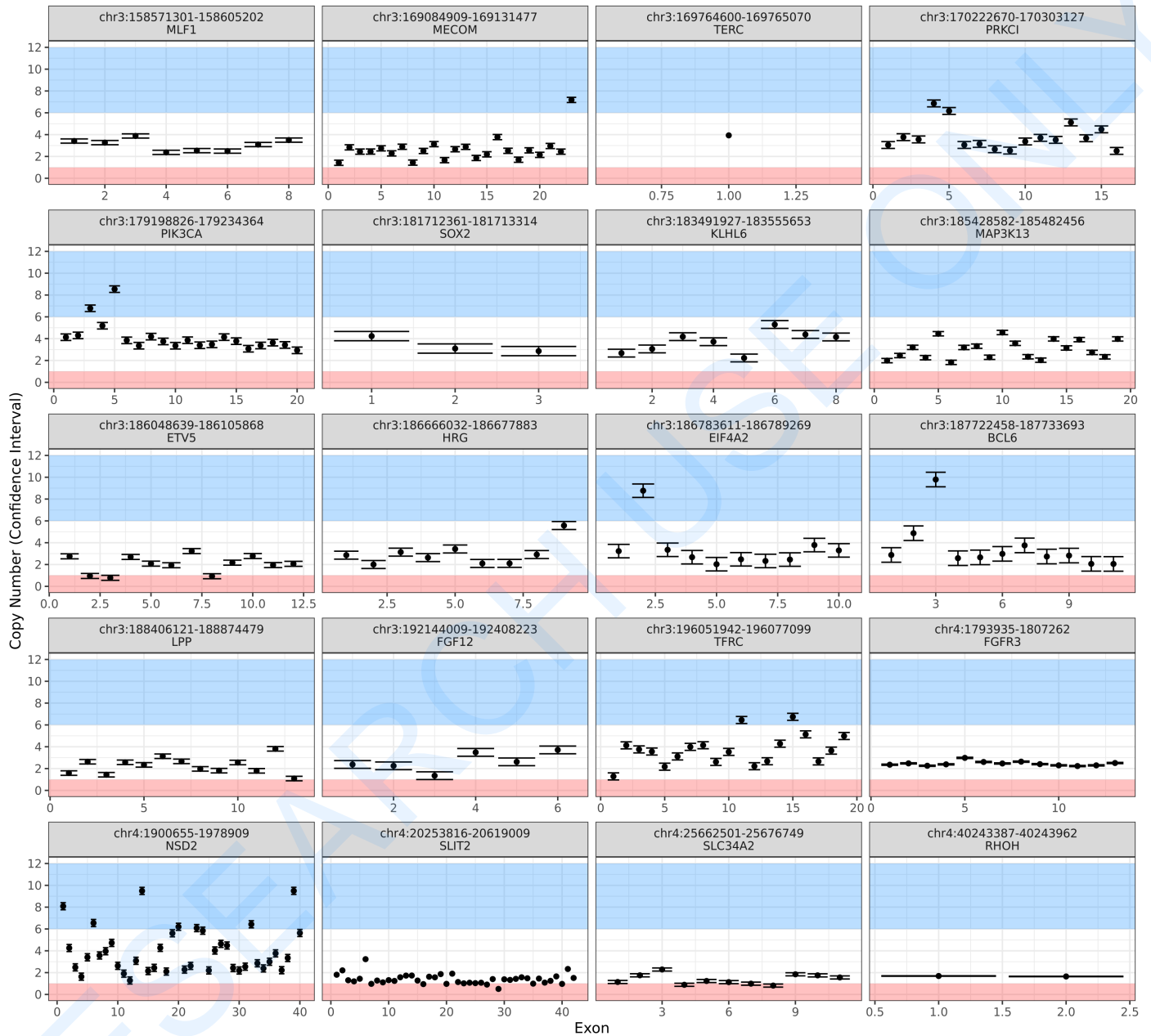


Copy number alterations by whole exome sequencing (WES):

The following plots provide estimated copy number values (black circle, y-axis) of exons per gene (x-axis), organized by chromosome (grey headers). Respective confidence intervals of each copy number call is also plotted for examining statistical error associated with next generation sequencing. Values are currently capped at 12 copies.



Copy Number Alterations

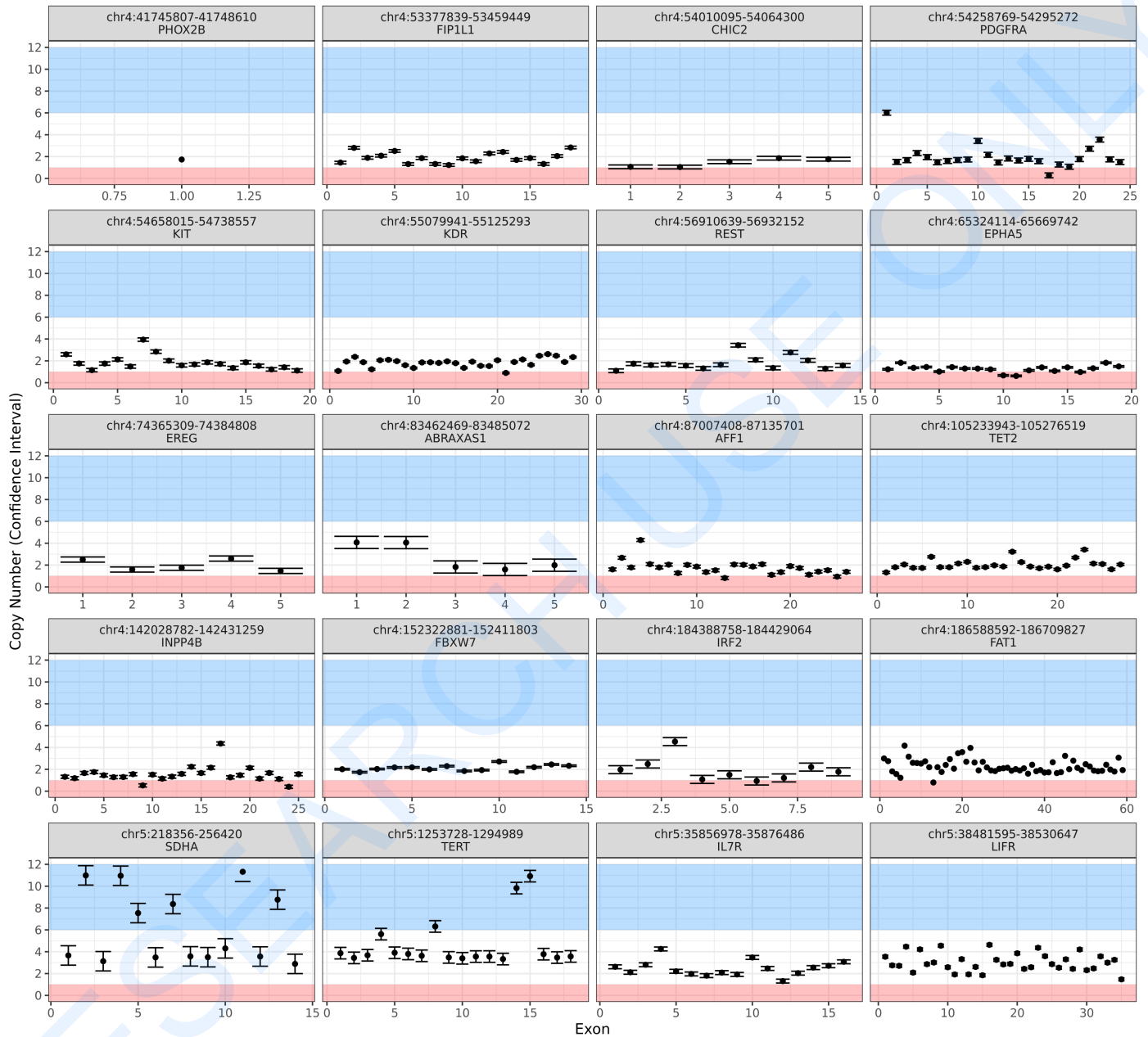


Copy number alterations by whole exome sequencing (WES):

The following plots provide estimated copy number values (black circle, y-axis) of exons per gene (x-axis), organized by chromosome (grey headers). Respective confidence intervals of each copy number call is also plotted for examining statistical error associated with next generation sequencing. Values are currently capped at 12 copies.



Copy Number Alterations

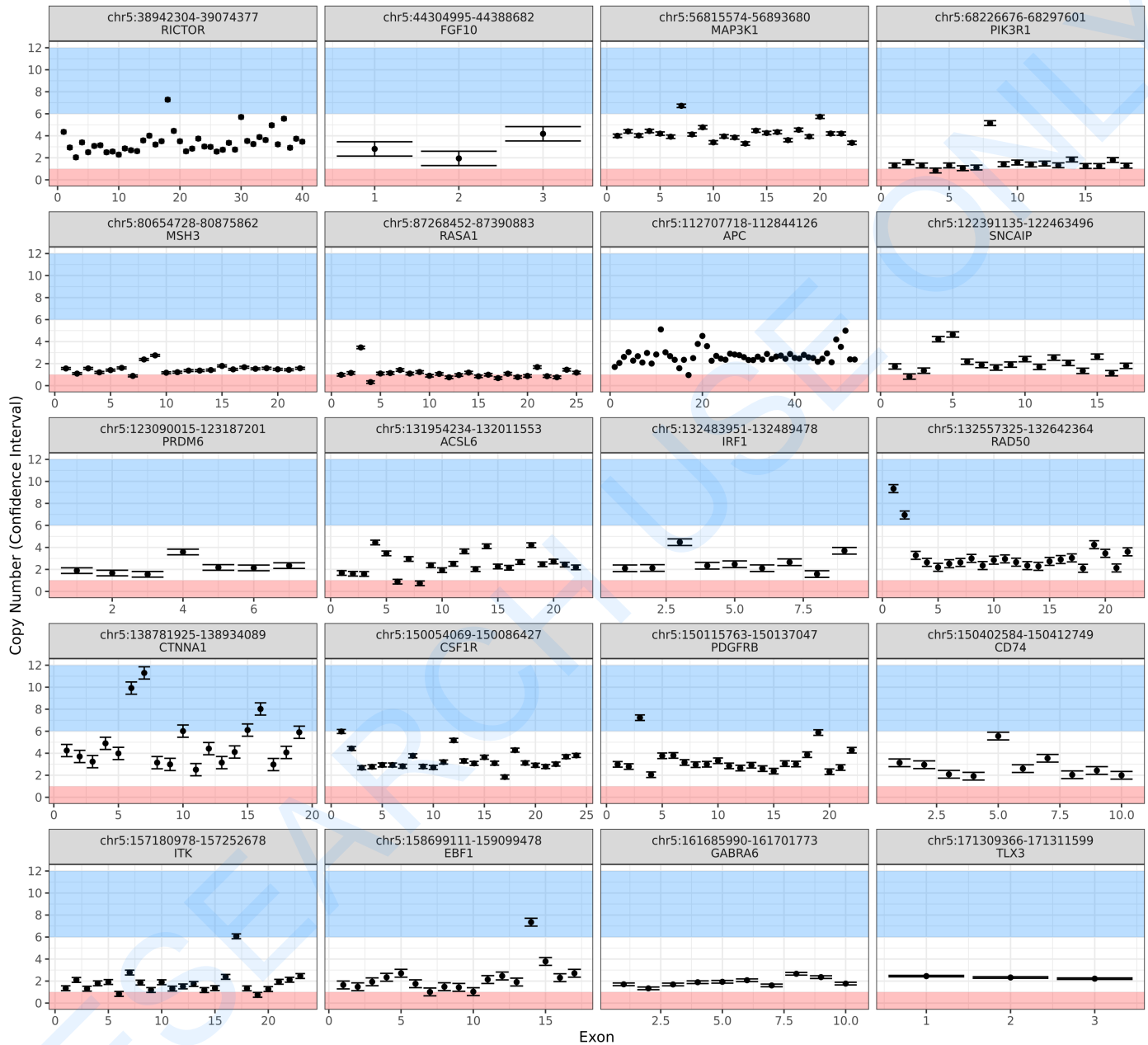


Copy number alterations by whole exome sequencing (WES):

The following plots provide estimated copy number values (black circle, y-axis) of exons per gene (x-axis), organized by chromosome (grey headers). Respective confidence intervals of each copy number call is also plotted for examining statistical error associated with next generation sequencing. Values are currently capped at 12 copies.



Copy Number Alterations

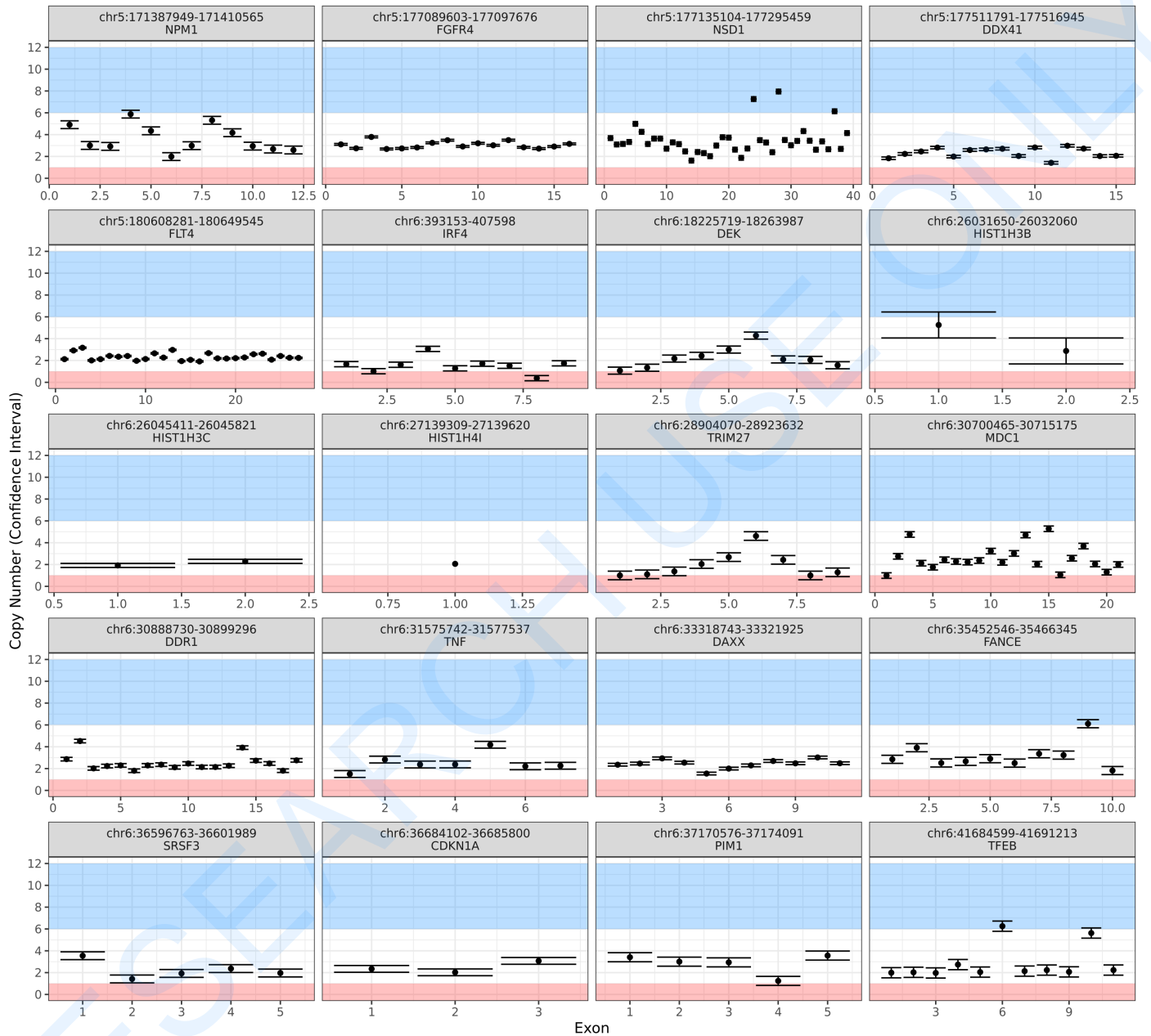


Copy number alterations by whole exome sequencing (WES):

The following plots provide estimated copy number values (black circle, y-axis) of exons per gene (x-axis), organized by chromosome (grey headers). Respective confidence intervals of each copy number call is also plotted for examining statistical error associated with next generation sequencing. Values are currently capped at 12 copies.



Copy Number Alterations

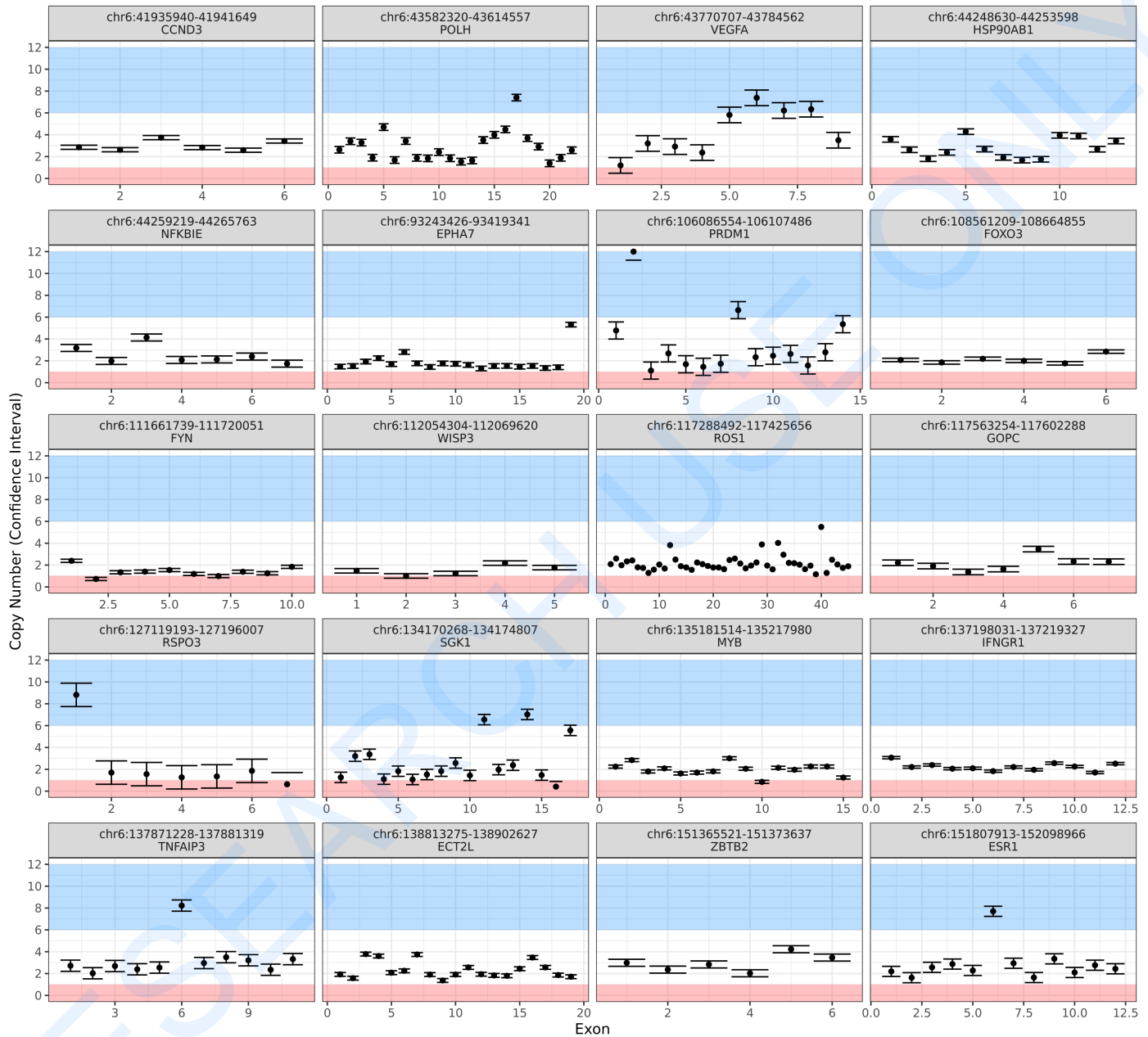


Copy number alterations by whole exome sequencing (WES):

The following plots provide estimated copy number values (black circle, y-axis) of exons per gene (x-axis), organized by chromosome (grey headers). Respective confidence intervals of each copy number call is also plotted for examining statistical error associated with next generation sequencing. Values are currently capped at 12 copies.



Copy Number Alterations

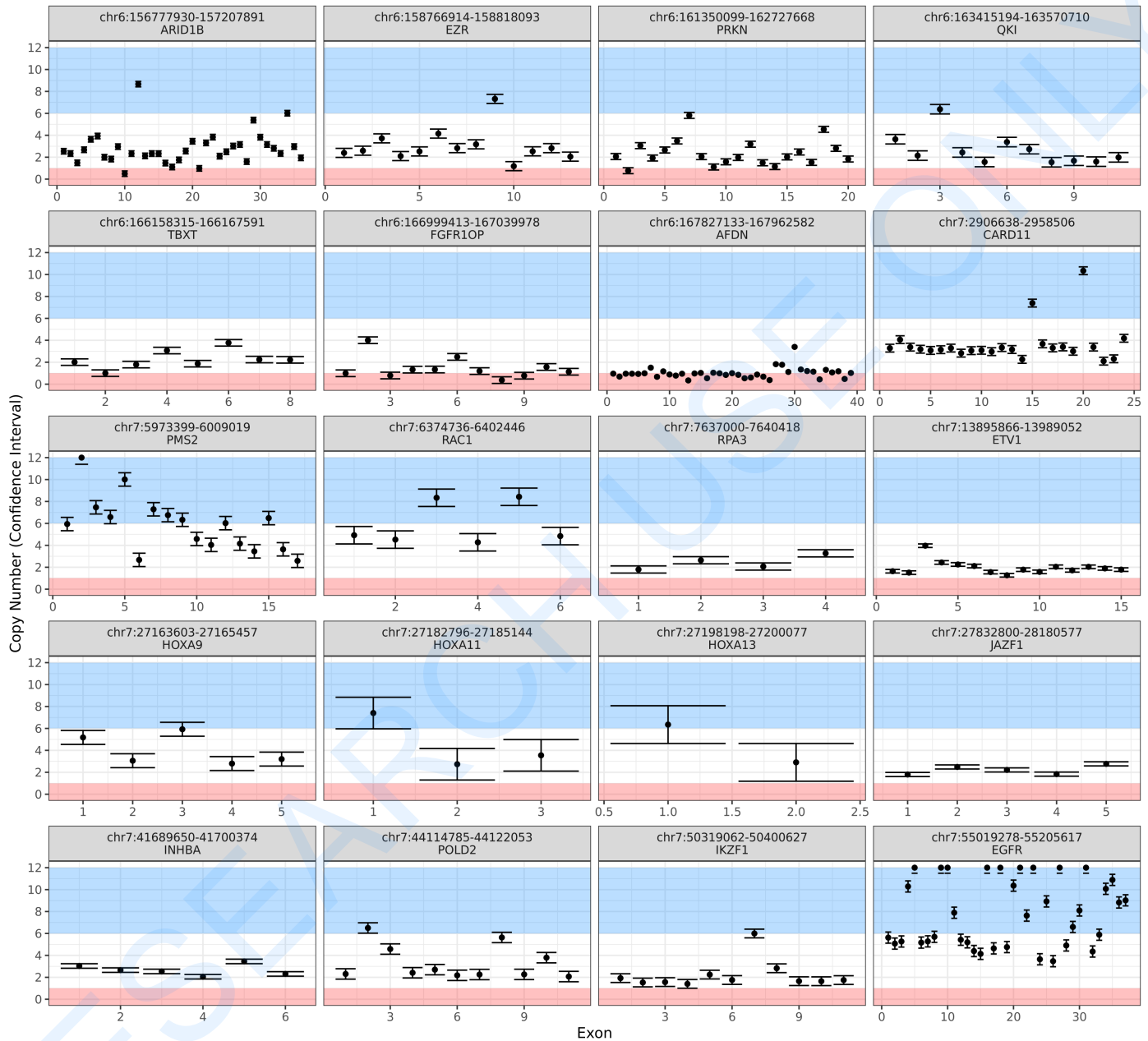


Copy number alterations by whole exome sequencing (WES):

The following plots provide estimated copy number values (black circle, y-axis) of exons per gene (x-axis), organized by chromosome (grey headers). Respective confidence intervals of each copy number call is also plotted for examining statistical error associated with next generation sequencing. Values are currently capped at 12 copies.



Copy Number Alterations

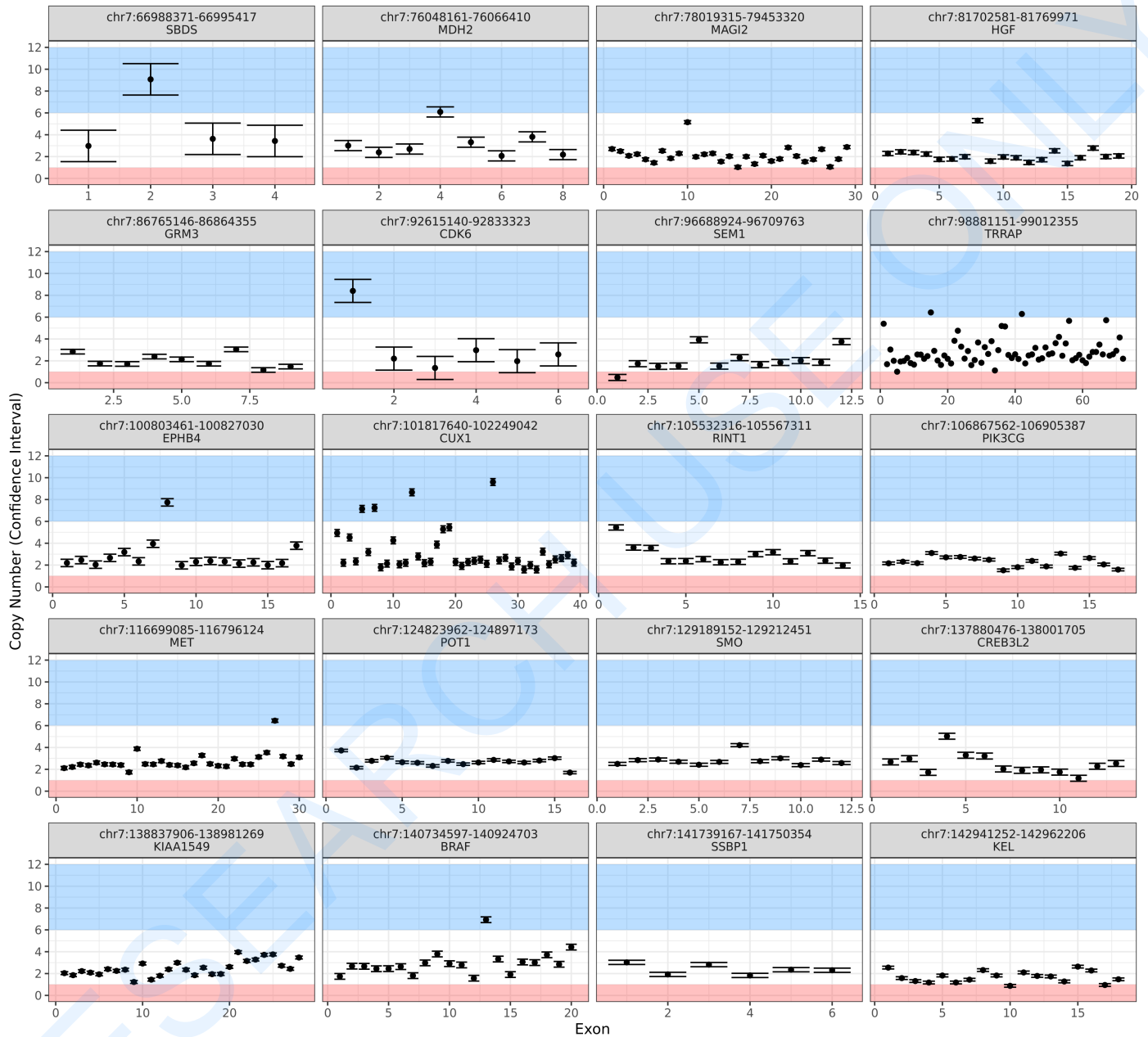


Copy number alterations by whole exome sequencing (WES):

The following plots provide estimated copy number values (black circle, y-axis) of exons per gene (x-axis), organized by chromosome (grey headers). Respective confidence intervals of each copy number call is also plotted for examining statistical error associated with next generation sequencing. Values are currently capped at 12 copies.



Copy Number Alterations

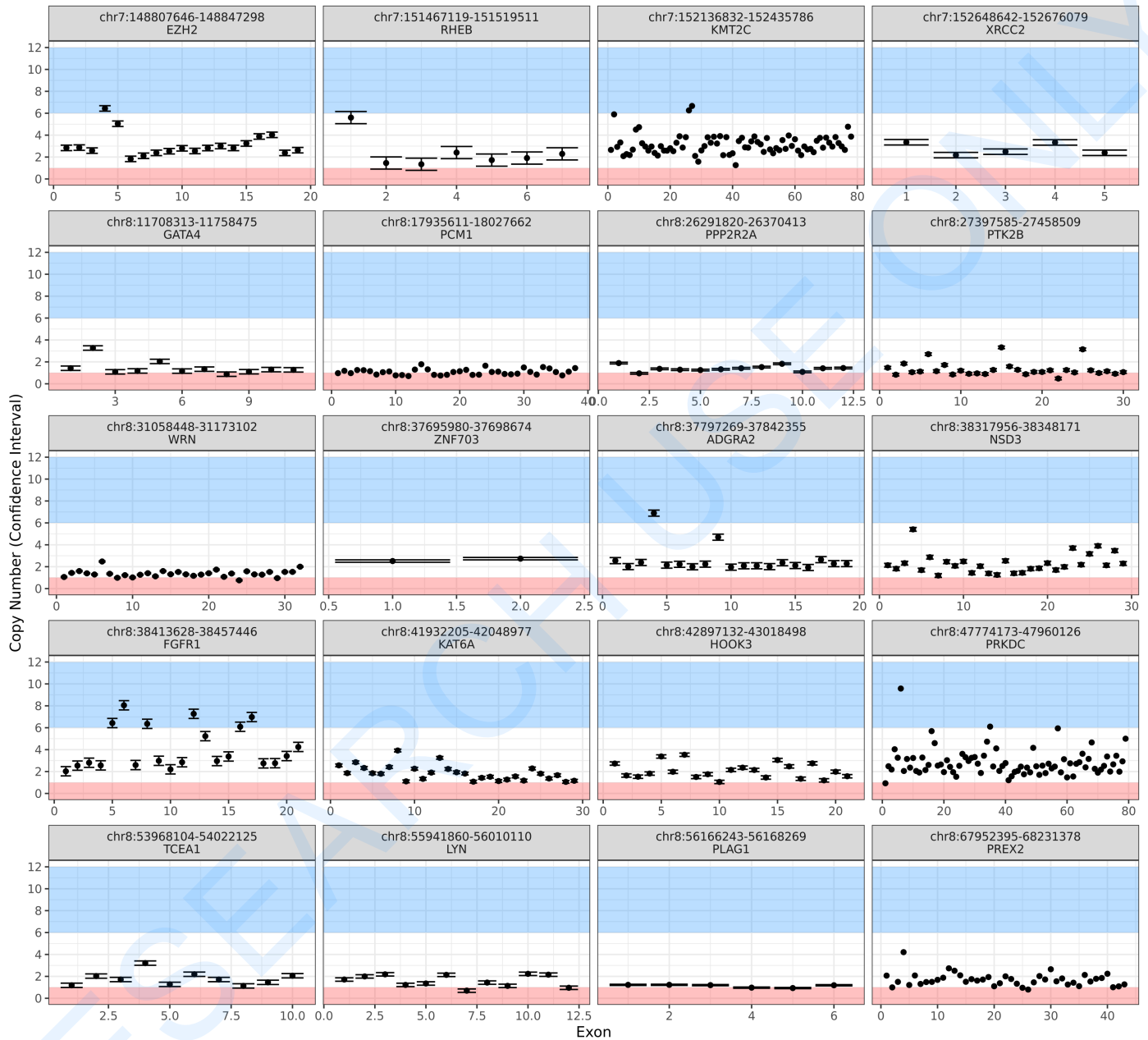


Copy number alterations by whole exome sequencing (WES):

The following plots provide estimated copy number values (black circle, y-axis) of exons per gene (x-axis), organized by chromosome (grey headers). Respective confidence intervals of each copy number call is also plotted for examining statistical error associated with next generation sequencing. Values are currently capped at 12 copies.



Copy Number Alterations

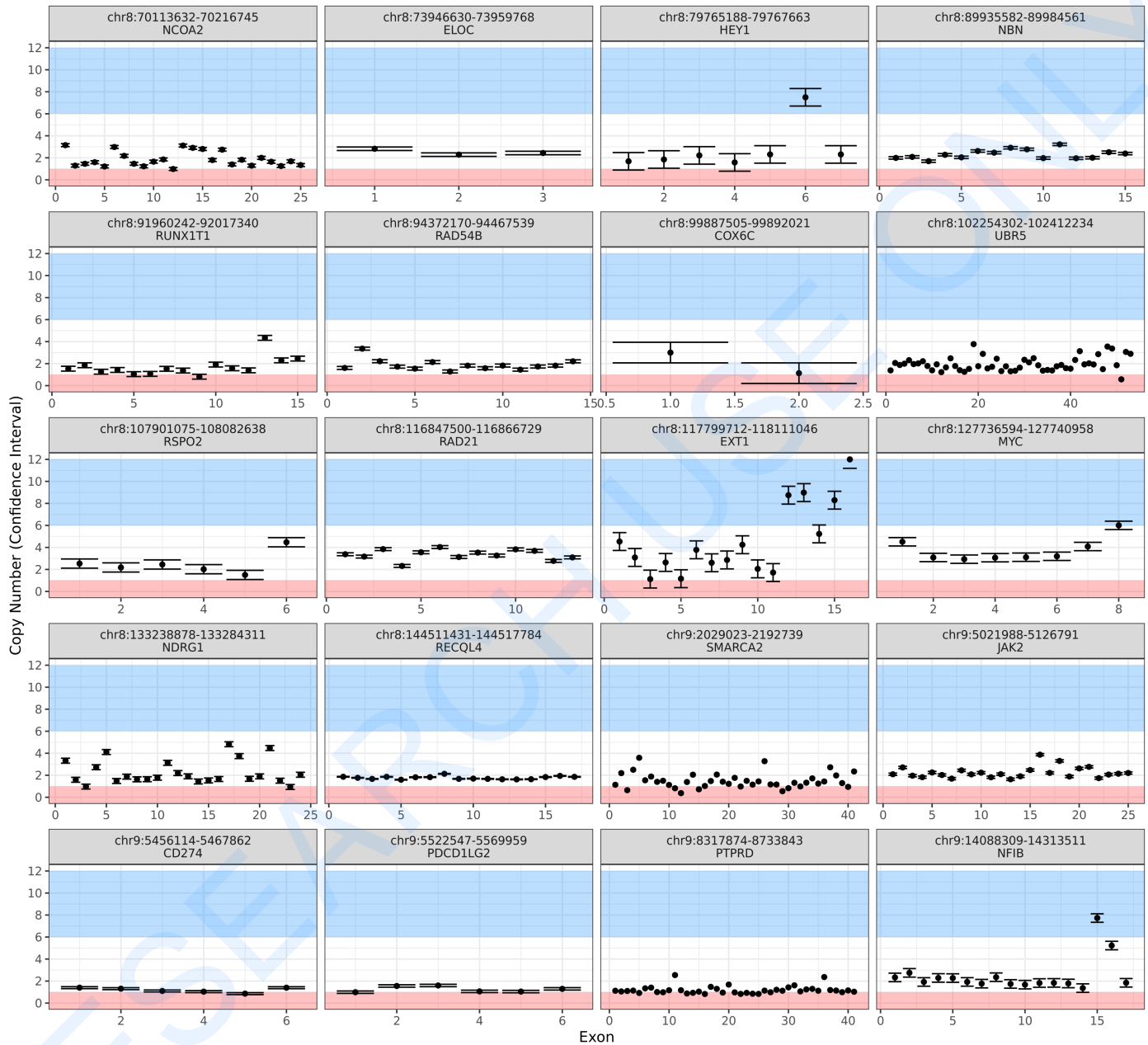


Copy number alterations by whole exome sequencing (WES):

The following plots provide estimated copy number values (black circle, y-axis) of exons per gene (x-axis), organized by chromosome (grey headers). Respective confidence intervals of each copy number call is also plotted for examining statistical error associated with next generation sequencing. Values are currently capped at 12 copies.



Copy Number Alterations

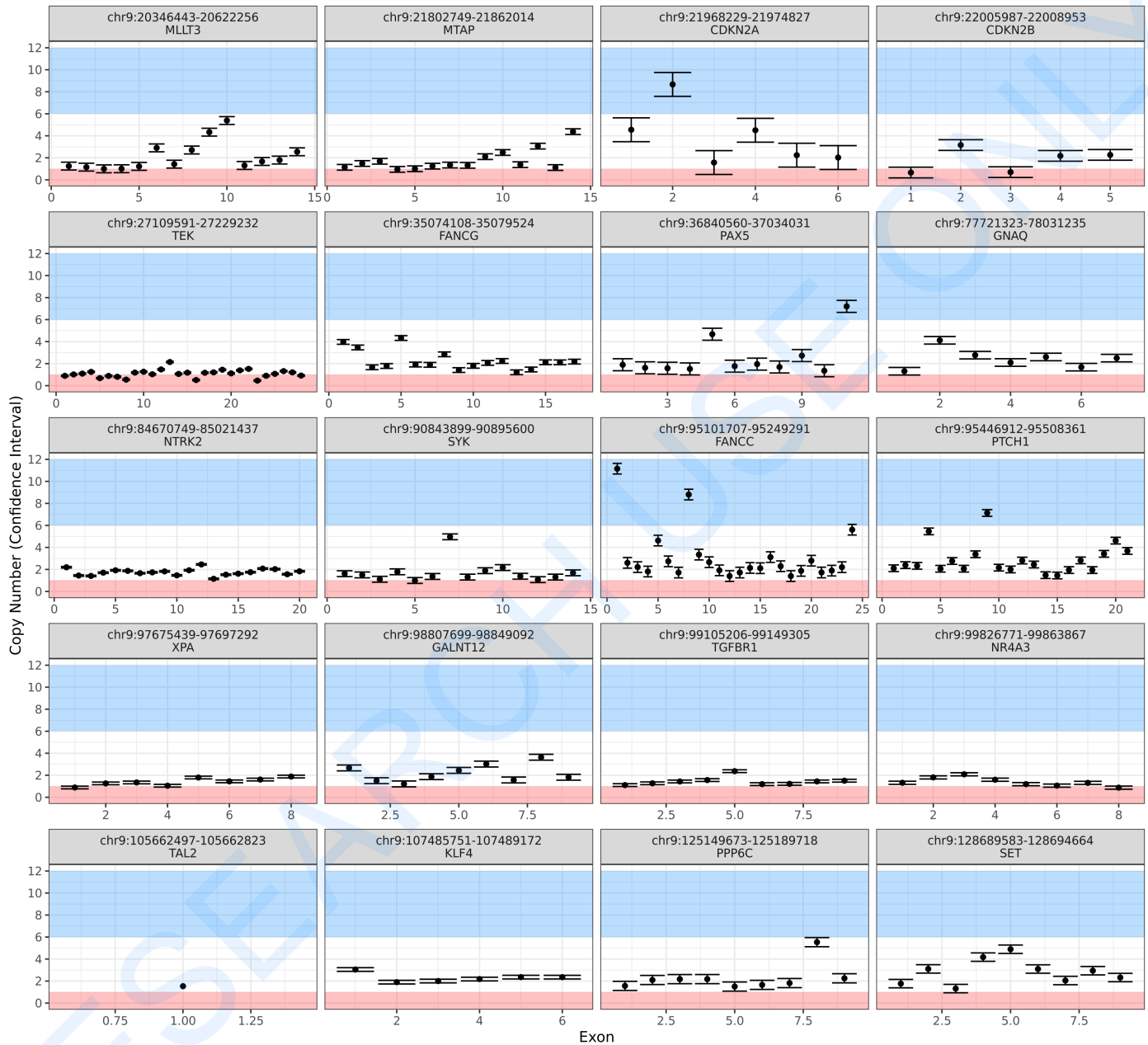


Copy number alterations by whole exome sequencing (WES):

The following plots provide estimated copy number values (black circle, y-axis) of exons per gene (x-axis), organized by chromosome (grey headers). Respective confidence intervals of each copy number call is also plotted for examining statistical error associated with next generation sequencing. Values are currently capped at 12 copies.



Copy Number Alterations

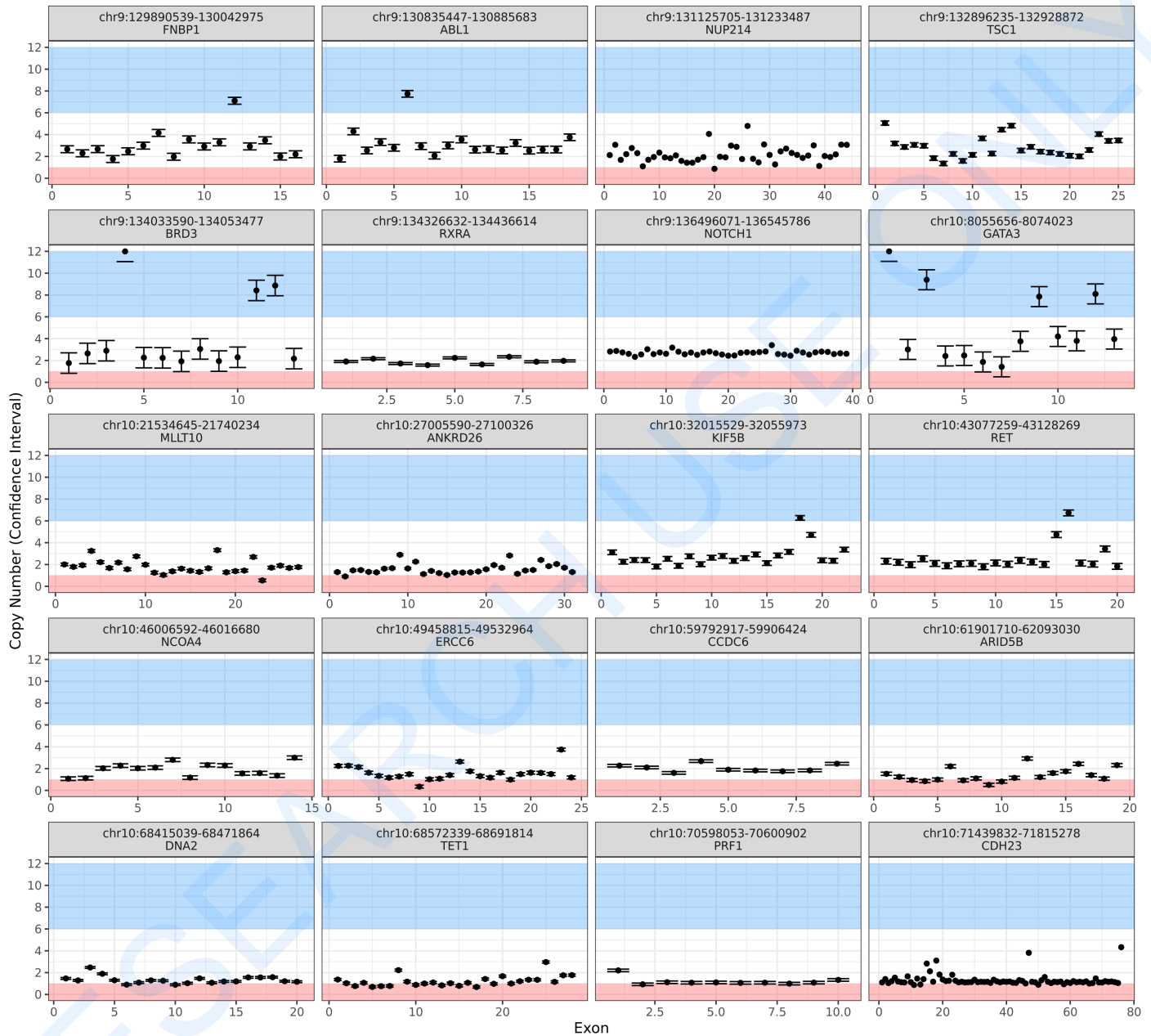


Copy number alterations by whole exome sequencing (WES):

The following plots provide estimated copy number values (black circle, y-axis) of exons per gene (x-axis), organized by chromosome (grey headers). Respective confidence intervals of each copy number call is also plotted for examining statistical error associated with next generation sequencing. Values are currently capped at 12 copies.



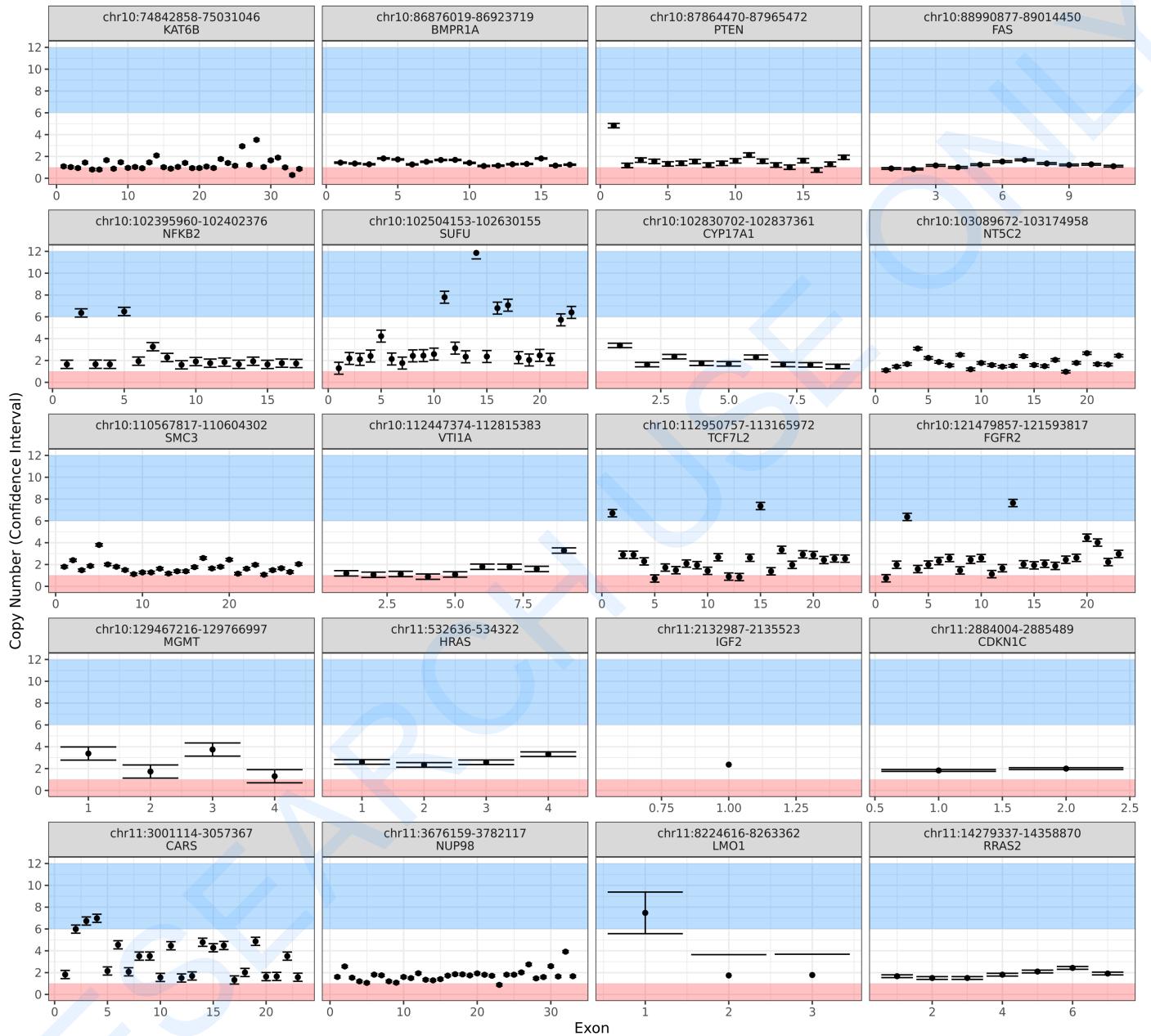
Copy Number Alterations



Copy number alterations by whole exome sequencing (WES):

The following plots provide estimated copy number values (black circle, y-axis) of exons per gene (x-axis), organized by chromosome (grey headers). Respective confidence intervals of each copy number call is also plotted for examining statistical error associated with next generation sequencing. Values are currently capped at 12 copies.

Copy Number Alterations

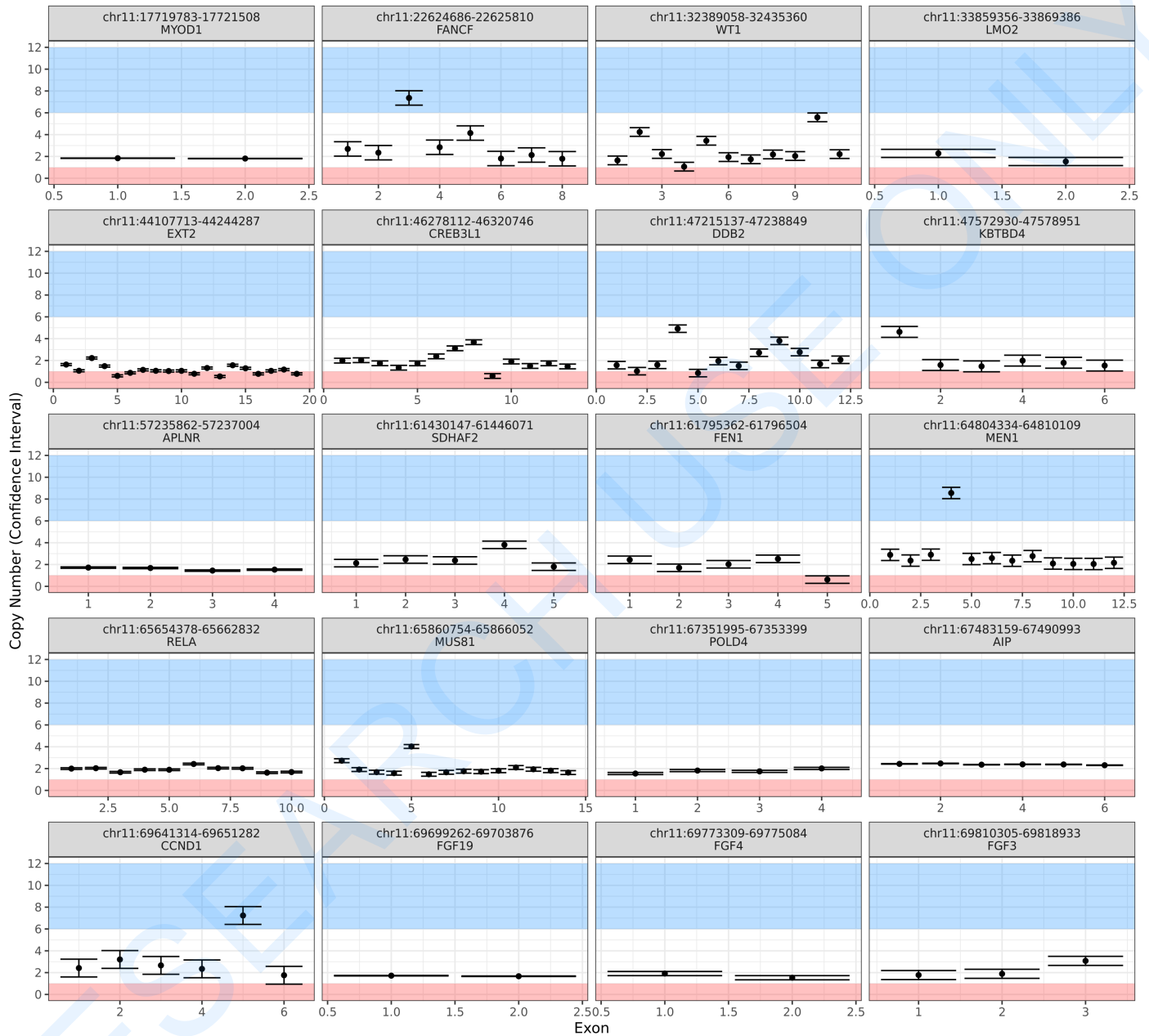


Copy number alterations by whole exome sequencing (WES):

The following plots provide estimated copy number values (black circle, y-axis) of exons per gene (x-axis), organized by chromosome (grey headers). Respective confidence intervals of each copy number call is also plotted for examining statistical error associated with next generation sequencing. Values are currently capped at 12 copies.



Copy Number Alterations

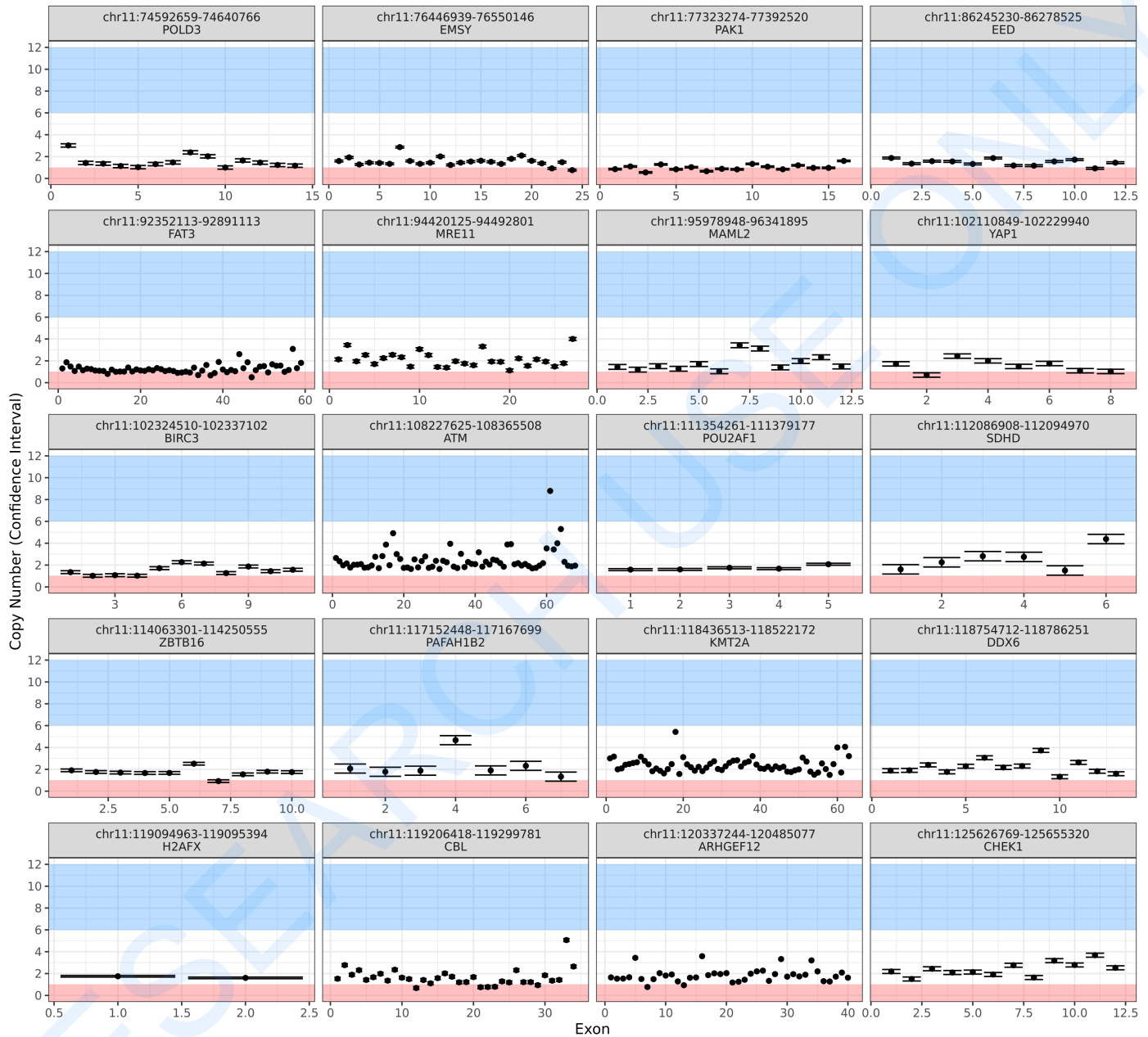


Copy number alterations by whole exome sequencing (WES):

The following plots provide estimated copy number values (black circle, y-axis) of exons per gene (x-axis), organized by chromosome (grey headers). Respective confidence intervals of each copy number call is also plotted for examining statistical error associated with next generation sequencing. Values are currently capped at 12 copies.



Copy Number Alterations

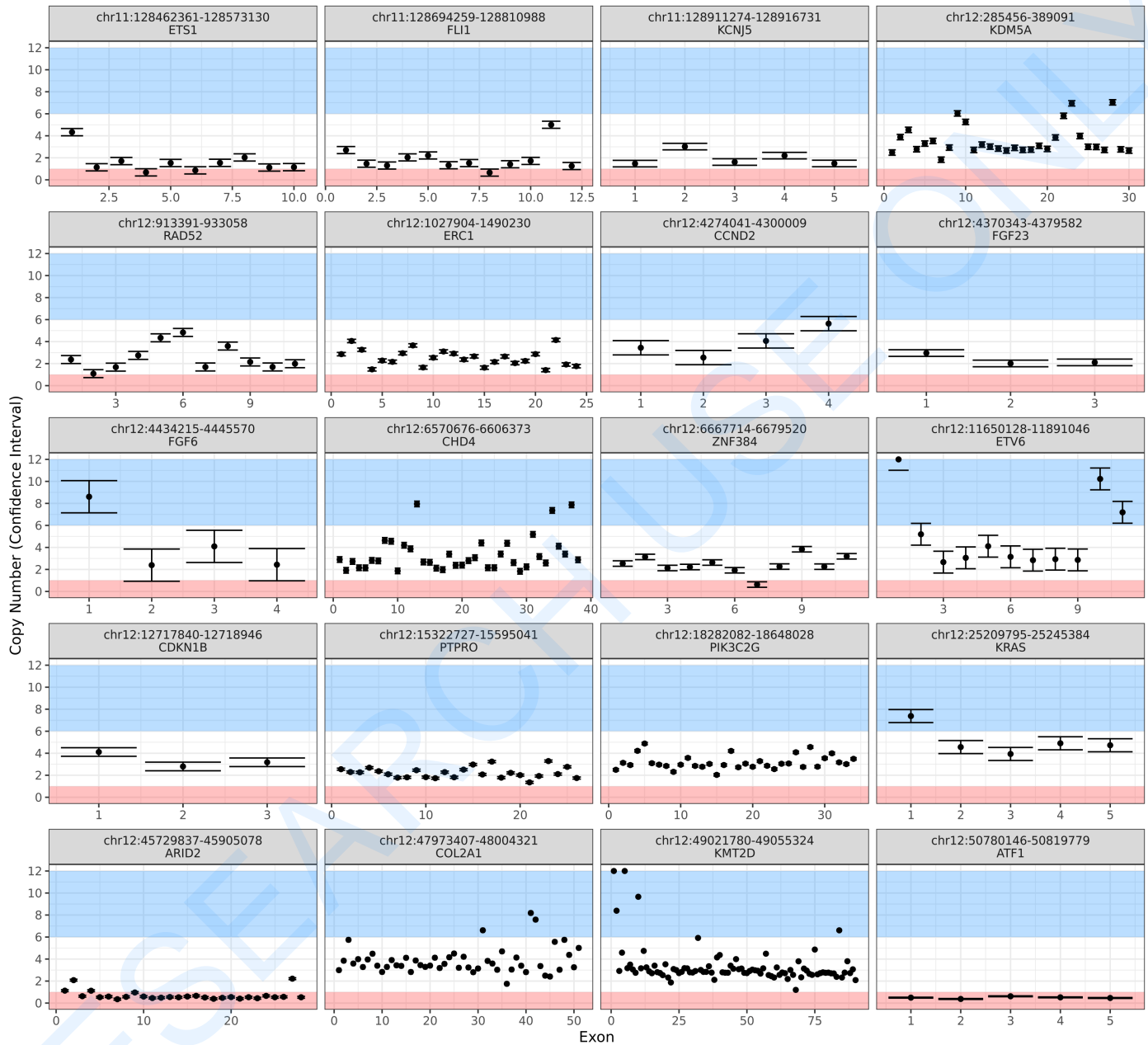


Copy number alterations by whole exome sequencing (WES):

The following plots provide estimated copy number values (black circle, y-axis) of exons per gene (x-axis), organized by chromosome (grey headers). Respective confidence intervals of each copy number call is also plotted for examining statistical error associated with next generation sequencing. Values are currently capped at 12 copies.



Copy Number Alterations

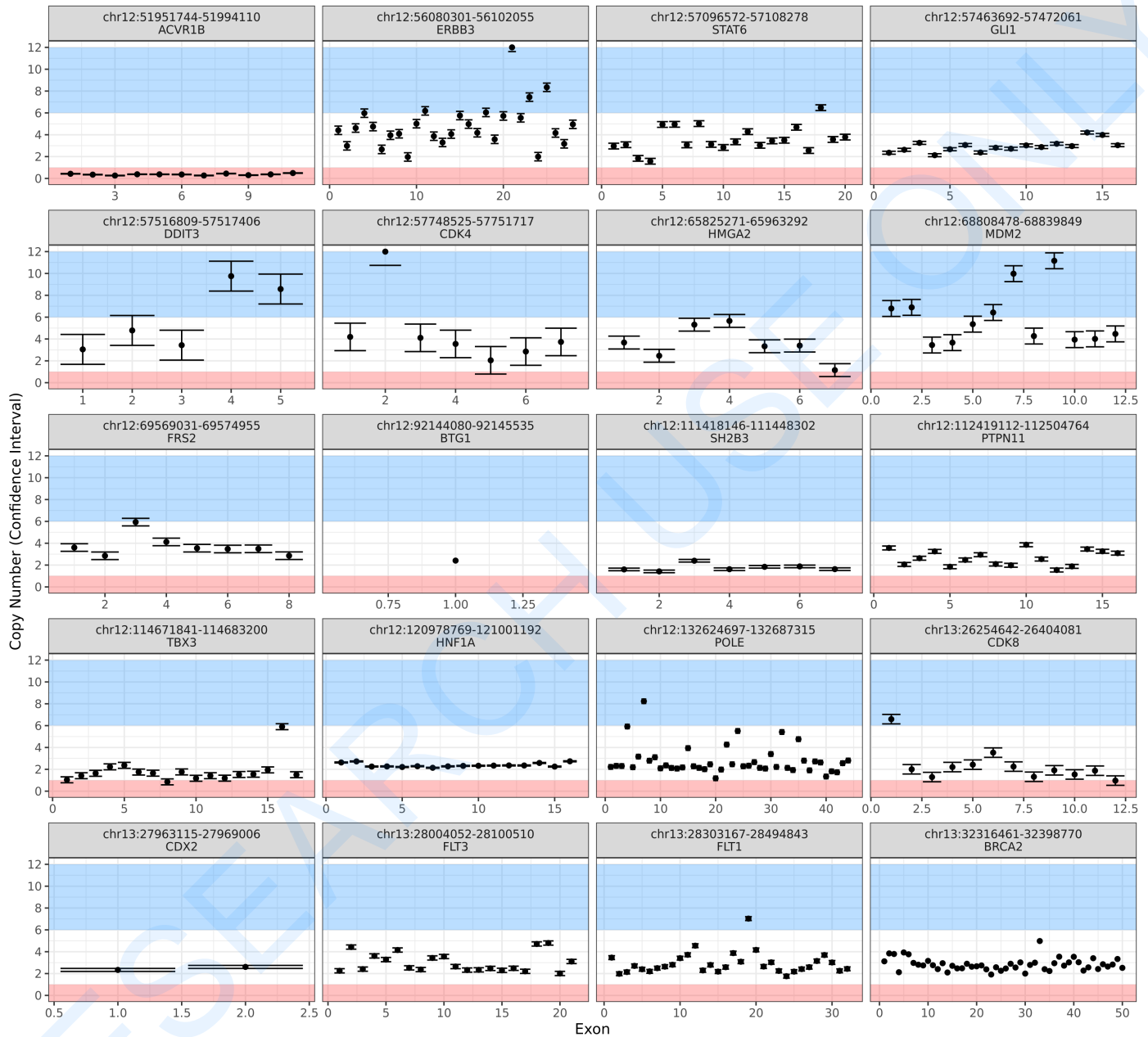


Copy number alterations by whole exome sequencing (WES):

The following plots provide estimated copy number values (black circle, y-axis) of exons per gene (x-axis), organized by chromosome (grey headers). Respective confidence intervals of each copy number call is also plotted for examining statistical error associated with next generation sequencing. Values are currently capped at 12 copies.



Copy Number Alterations

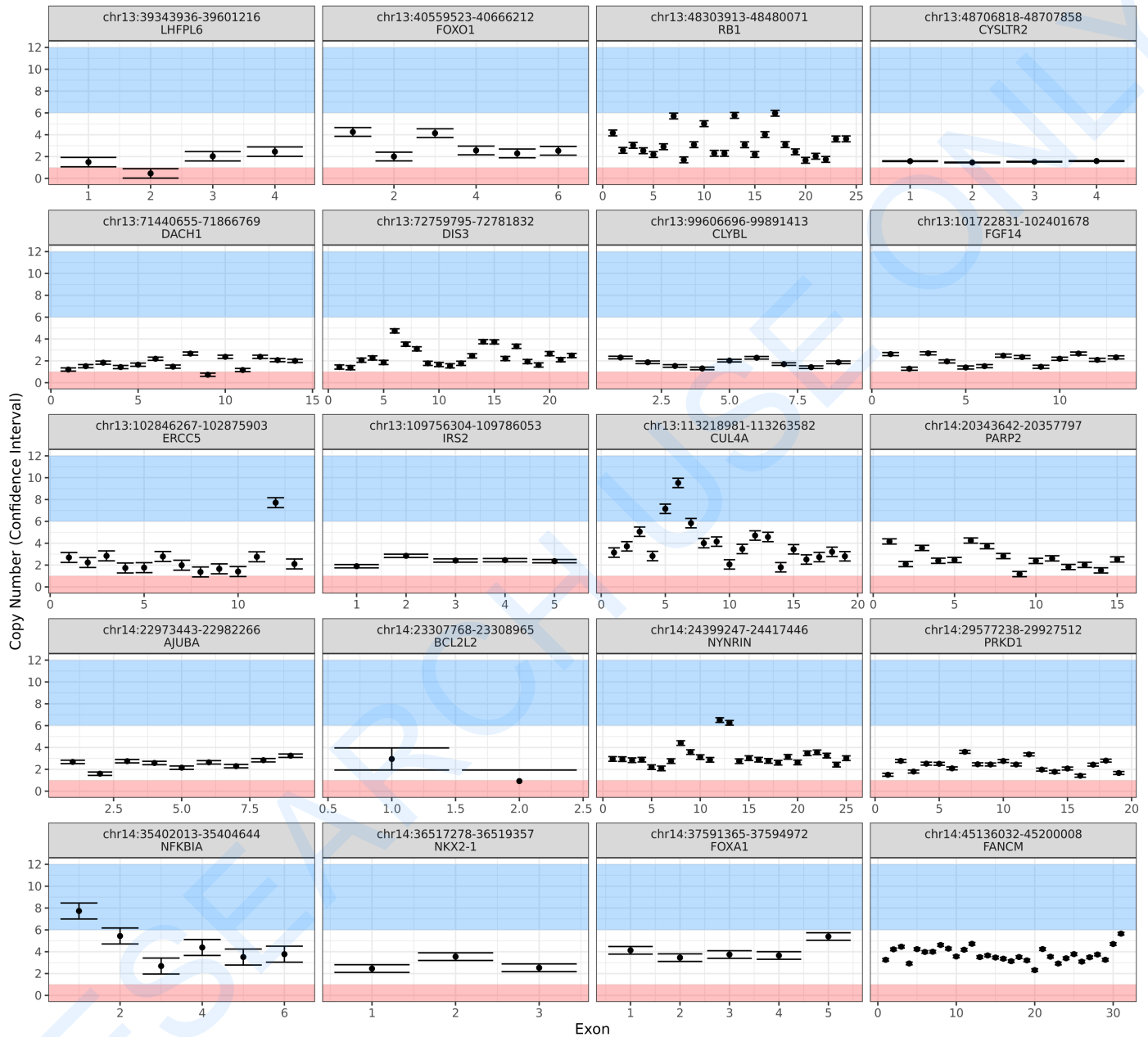


Copy number alterations by whole exome sequencing (WES):

The following plots provide estimated copy number values (black circle, y-axis) of exons per gene (x-axis), organized by chromosome (grey headers). Respective confidence intervals of each copy number call is also plotted for examining statistical error associated with next generation sequencing. Values are currently capped at 12 copies.



Copy Number Alterations

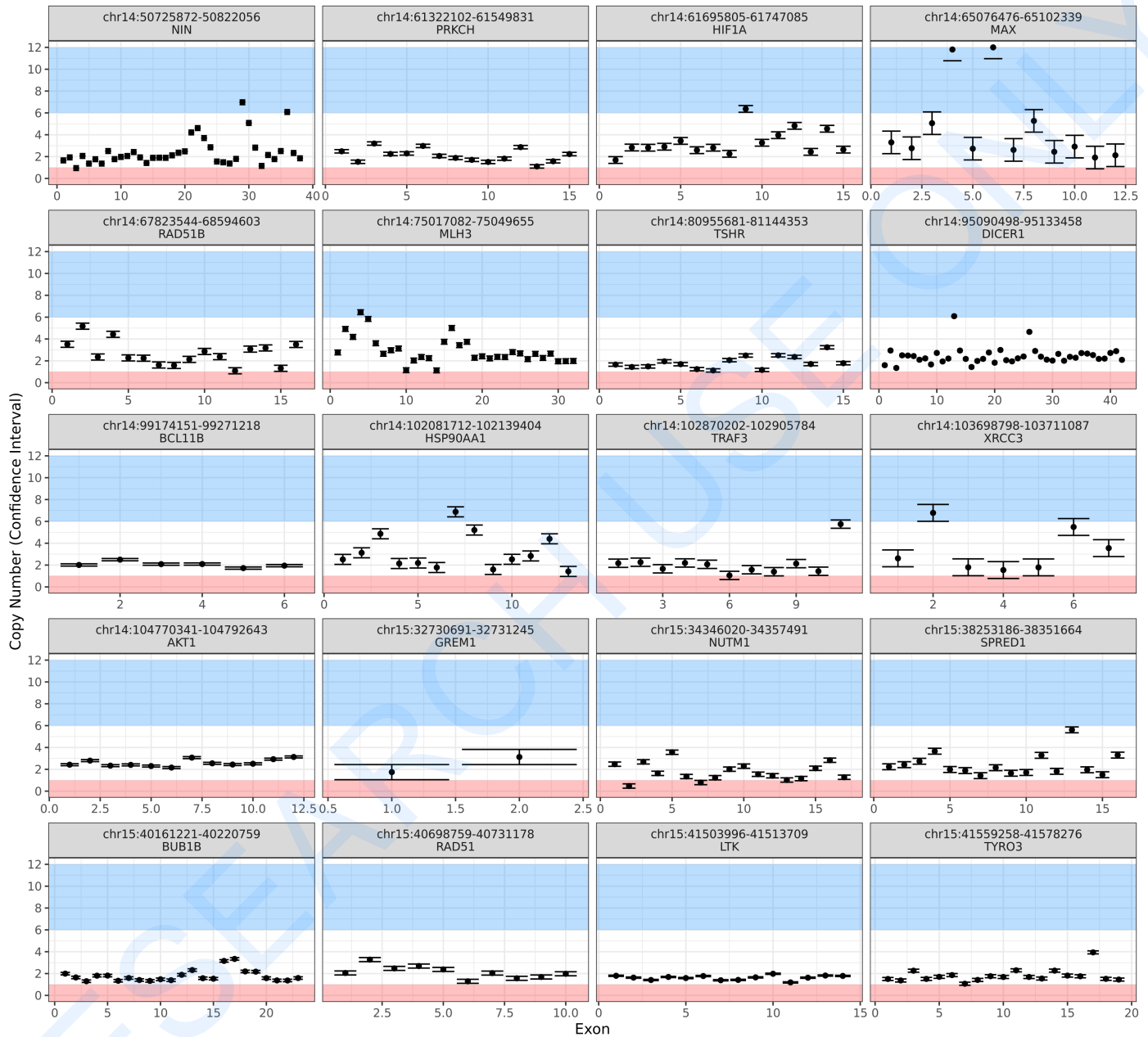


Copy number alterations by whole exome sequencing (WES):

The following plots provide estimated copy number values (black circle, y-axis) of exons per gene (x-axis), organized by chromosome (grey headers). Respective confidence intervals of each copy number call is also plotted for examining statistical error associated with next generation sequencing. Values are currently capped at 12 copies.



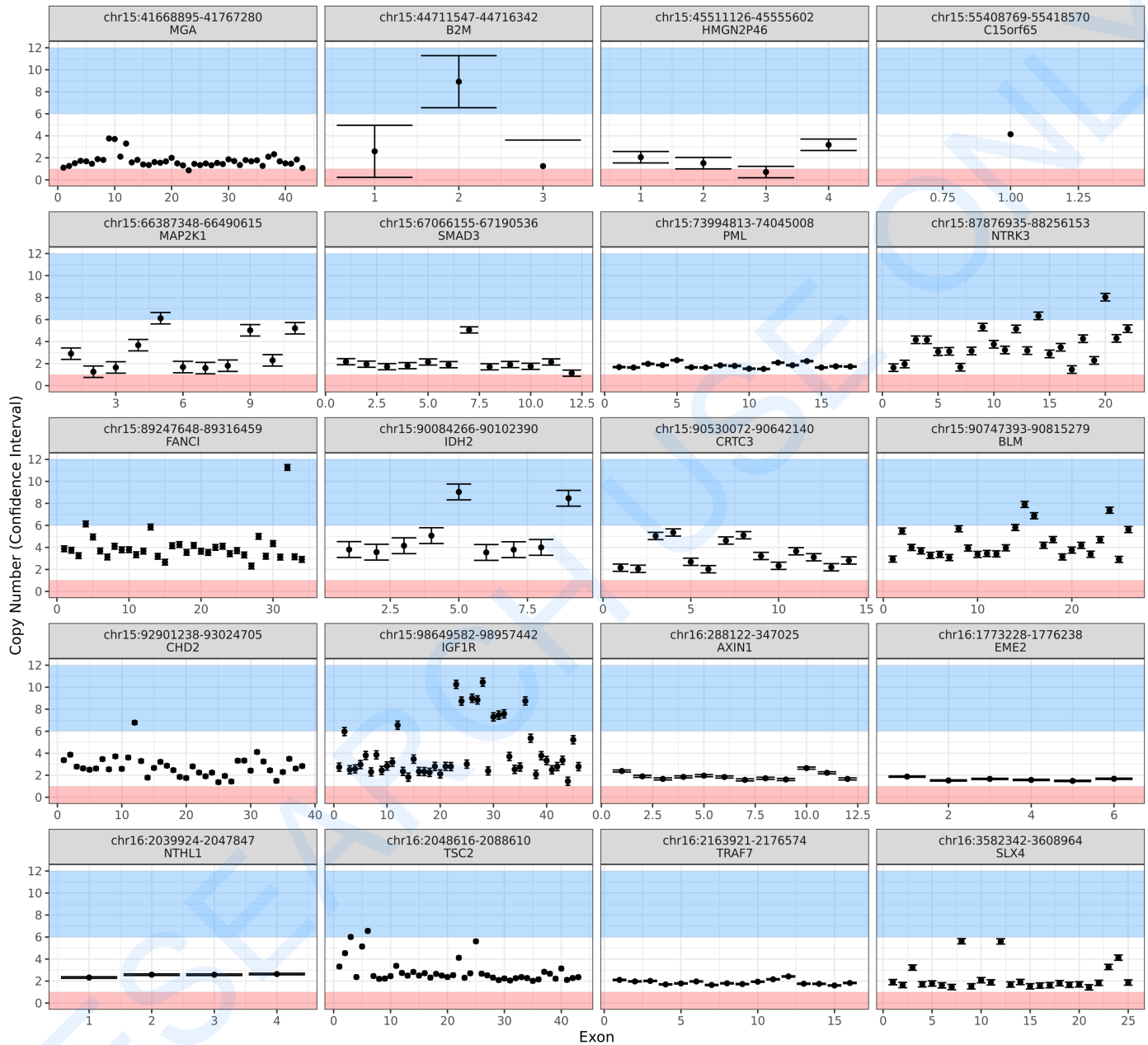
Copy Number Alterations



Copy number alterations by whole exome sequencing (WES):

The following plots provide estimated copy number values (black circle, y-axis) of exons per gene (x-axis), organized by chromosome (grey headers). Respective confidence intervals of each copy number call is also plotted for examining statistical error associated with next generation sequencing. Values are currently capped at 12 copies.

Copy Number Alterations

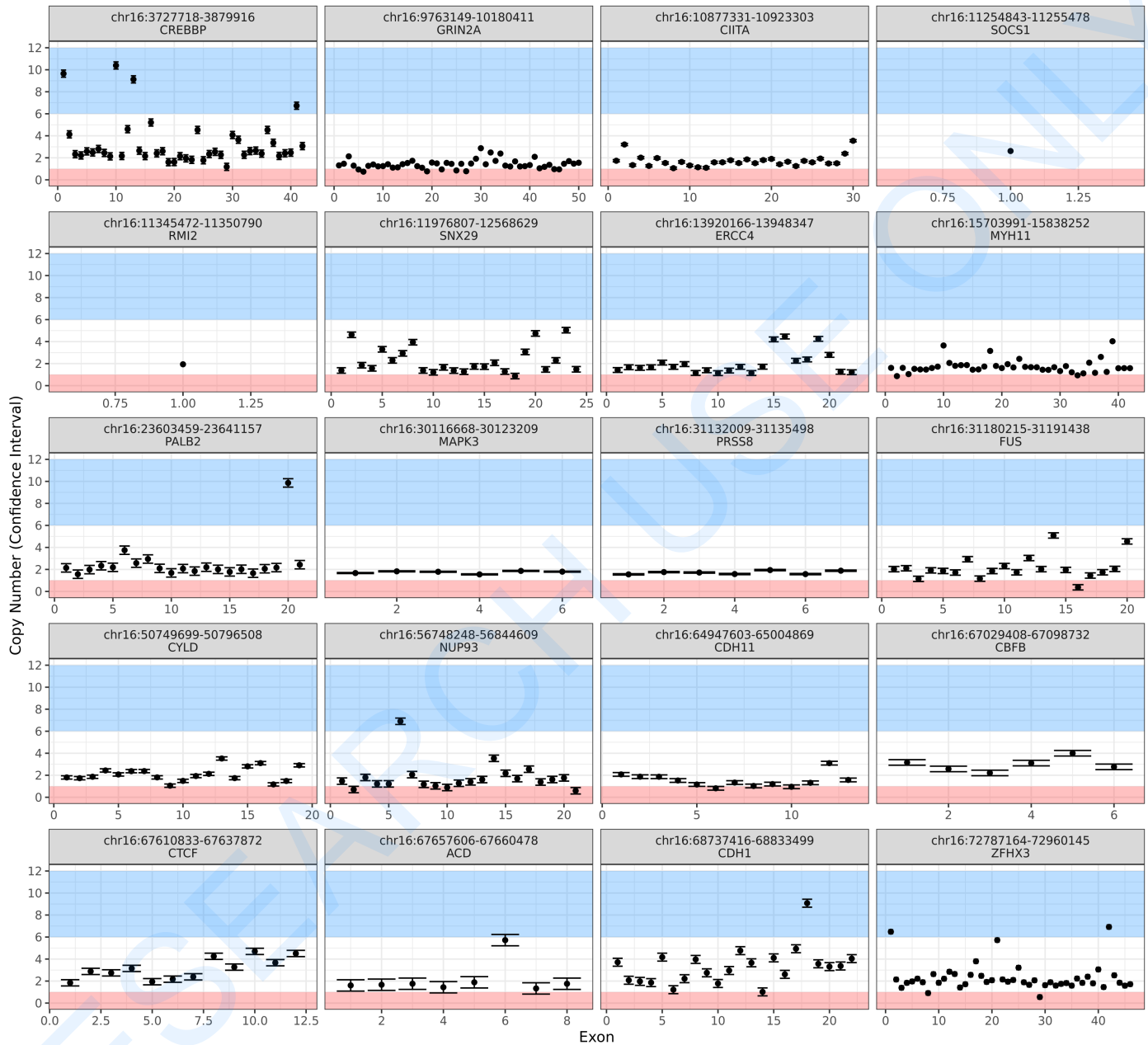


Copy number alterations by whole exome sequencing (WES):

The following plots provide estimated copy number values (black circle, y-axis) of exons per gene (x-axis), organized by chromosome (grey headers). Respective confidence intervals of each copy number call is also plotted for examining statistical error associated with next generation sequencing. Values are currently capped at 12 copies.



Copy Number Alterations

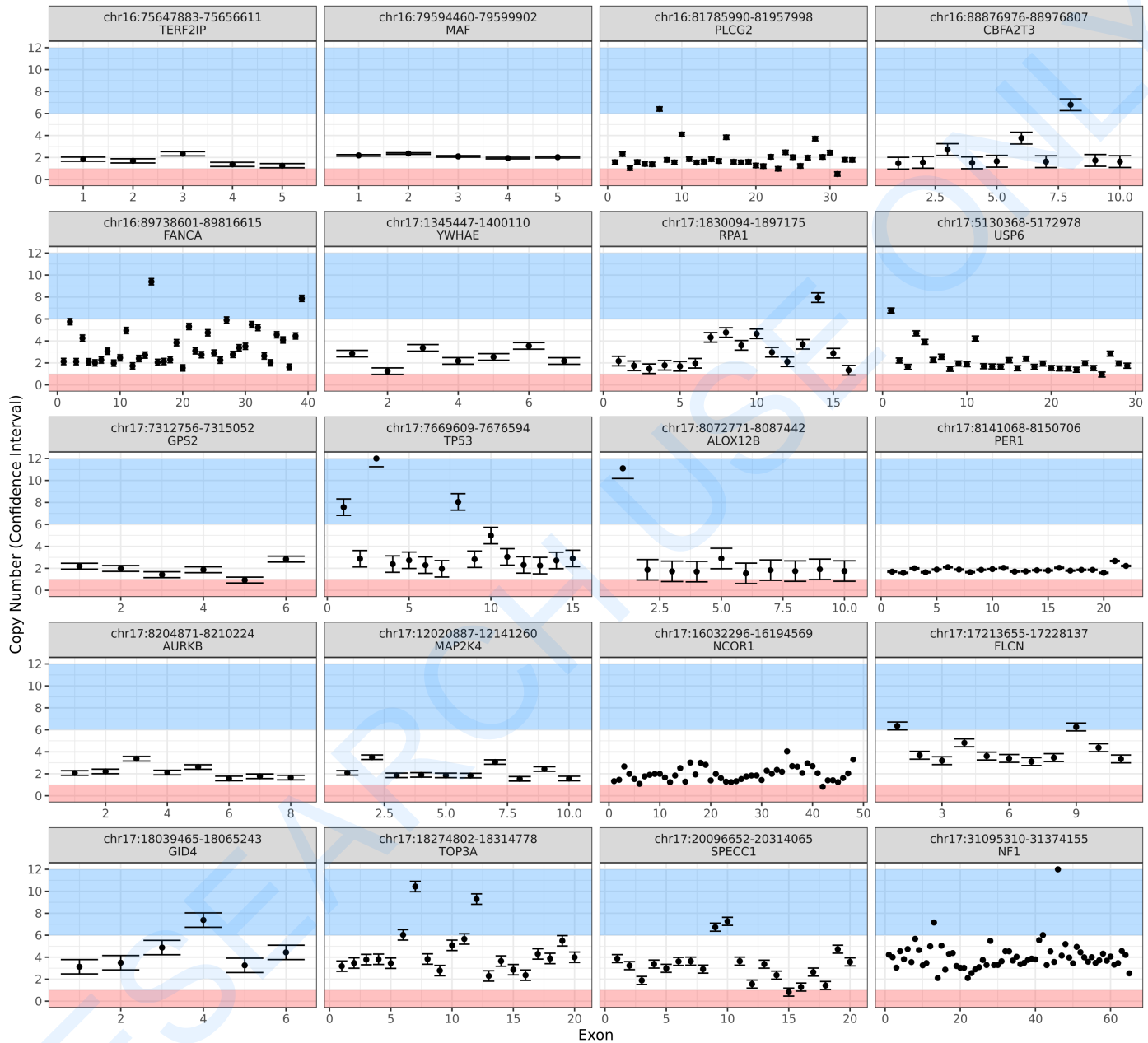


Copy number alterations by whole exome sequencing (WES):

The following plots provide estimated copy number values (black circle, y-axis) of exons per gene (x-axis), organized by chromosome (grey headers). Respective confidence intervals of each copy number call is also plotted for examining statistical error associated with next generation sequencing. Values are currently capped at 12 copies.



Copy Number Alterations

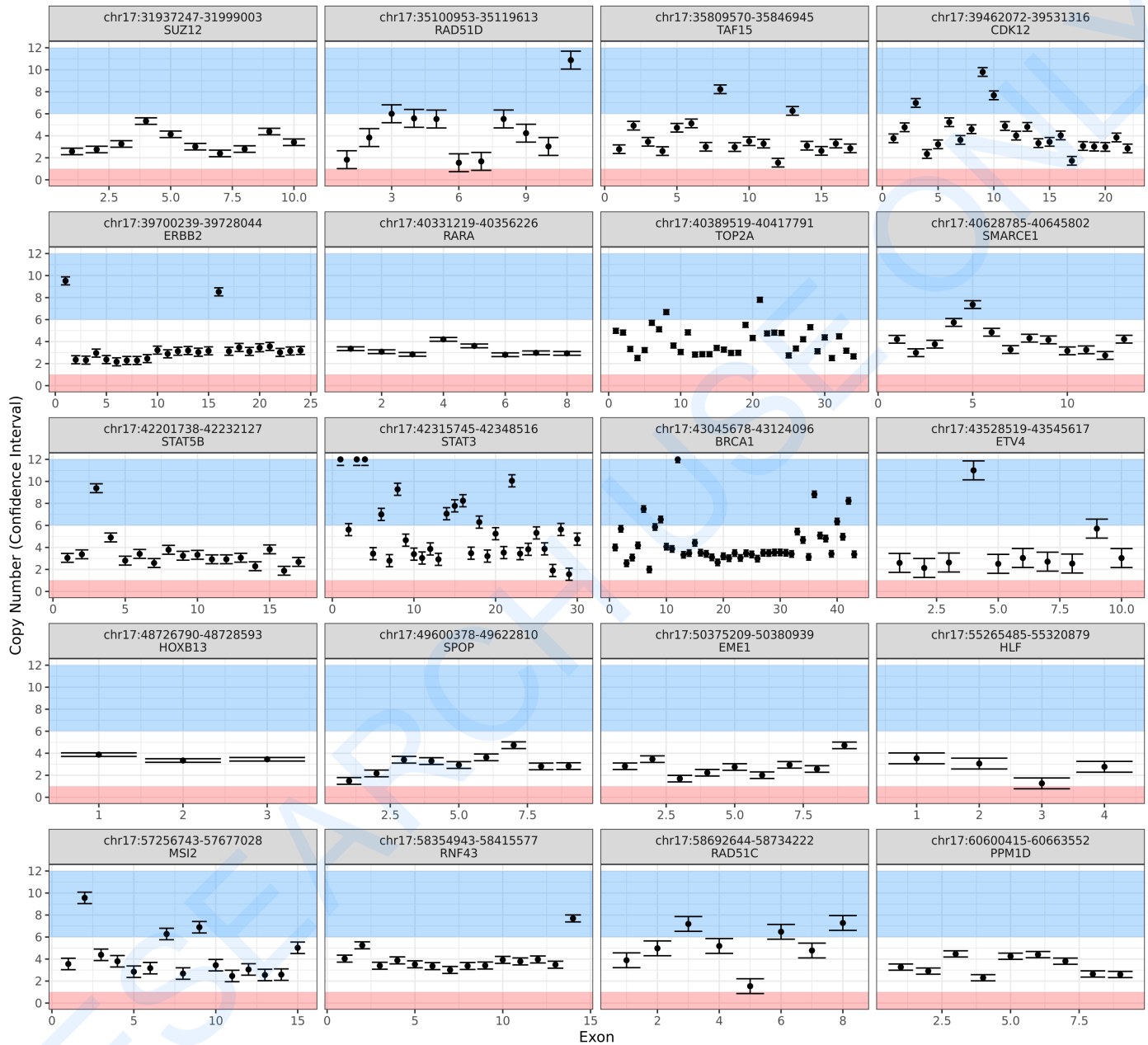


Copy number alterations by whole exome sequencing (WES):

The following plots provide estimated copy number values (black circle, y-axis) of exons per gene (x-axis), organized by chromosome (grey headers). Respective confidence intervals of each copy number call is also plotted for examining statistical error associated with next generation sequencing. Values are currently capped at 12 copies.



Copy Number Alterations

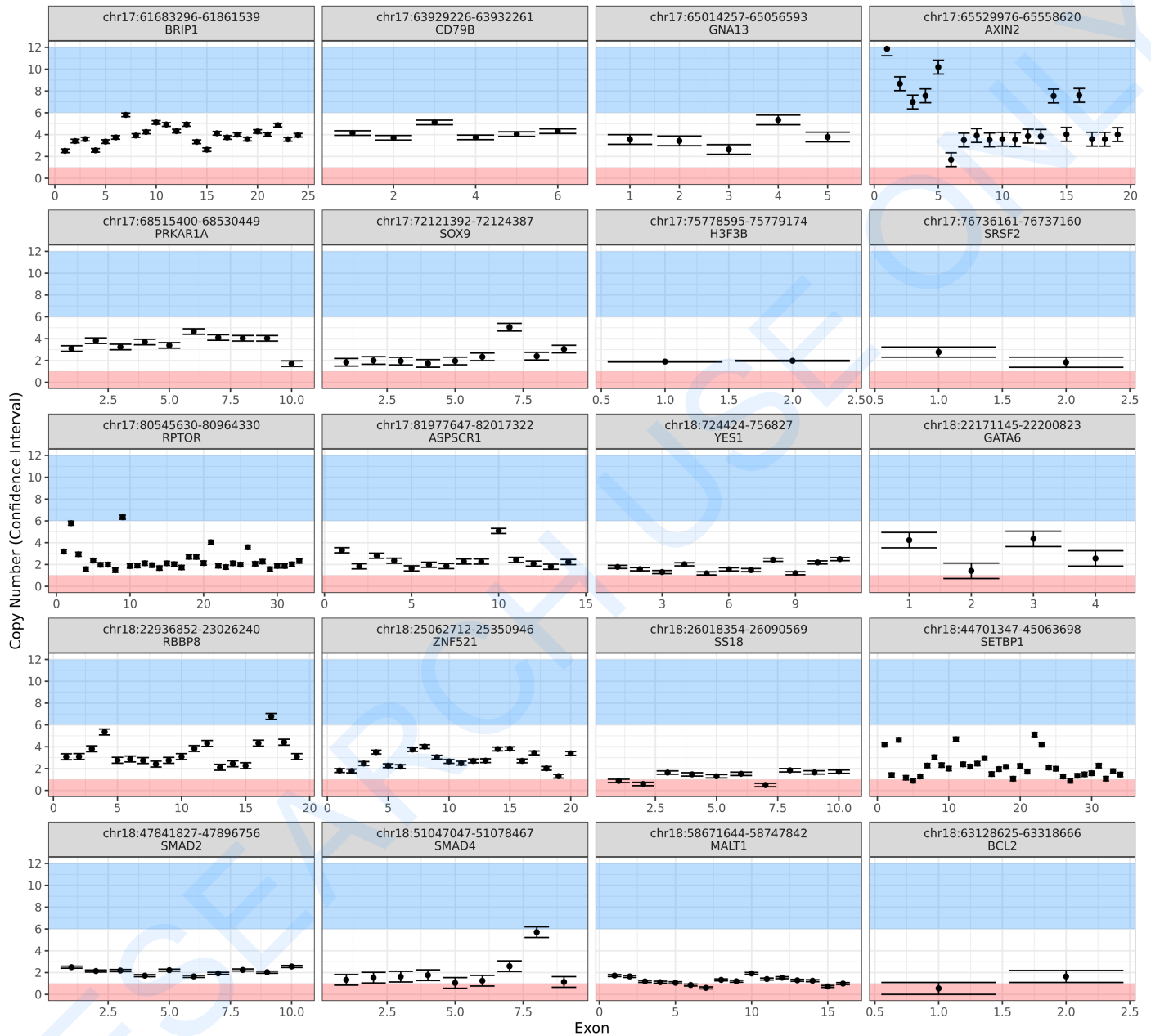


Copy number alterations by whole exome sequencing (WES):

The following plots provide estimated copy number values (black circle, y-axis) of exons per gene (x-axis), organized by chromosome (grey headers). Respective confidence intervals of each copy number call is also plotted for examining statistical error associated with next generation sequencing. Values are currently capped at 12 copies.



Copy Number Alterations

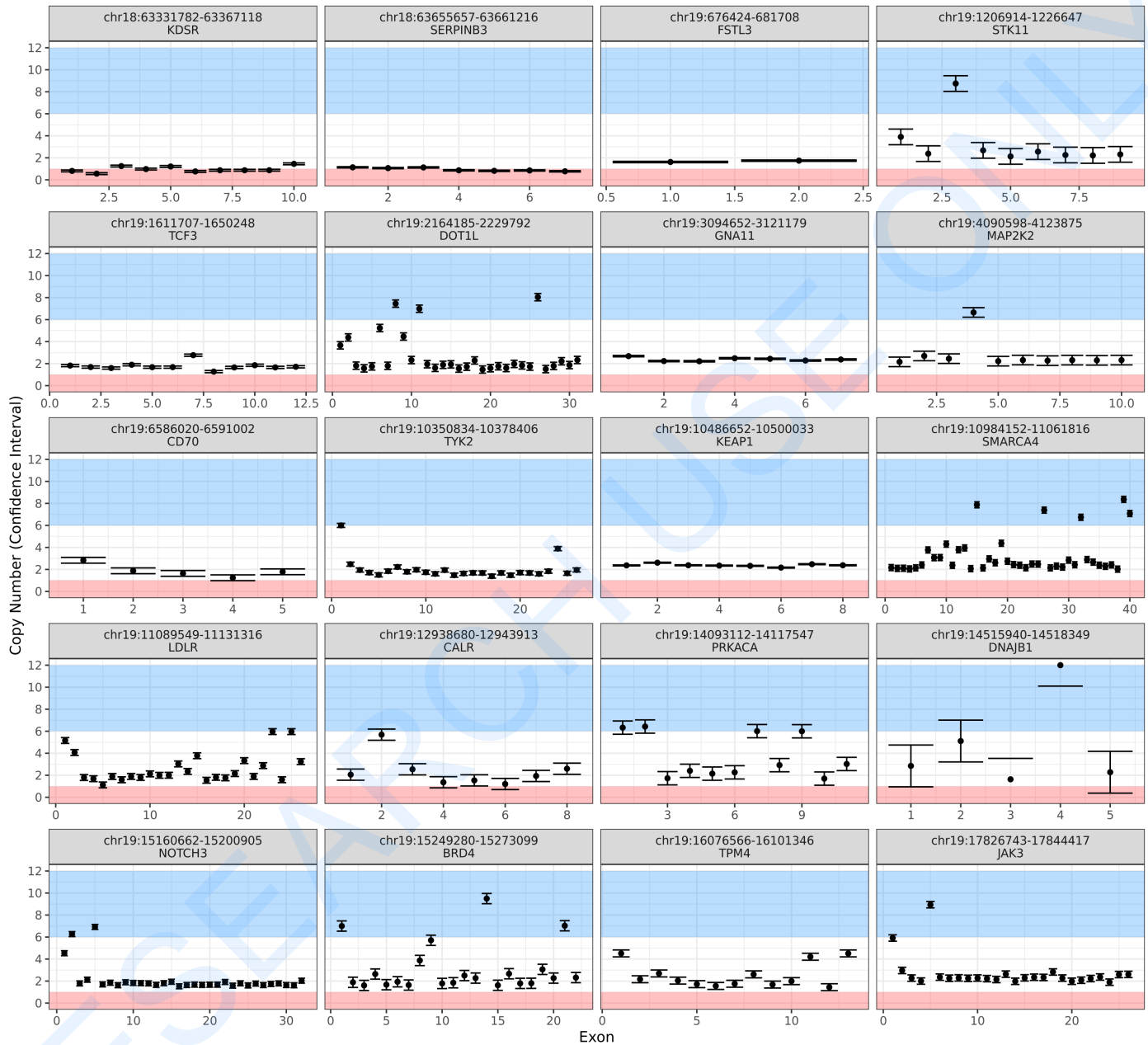


Copy number alterations by whole exome sequencing (WES):

The following plots provide estimated copy number values (black circle, y-axis) of exons per gene (x-axis), organized by chromosome (grey headers). Respective confidence intervals of each copy number call is also plotted for examining statistical error associated with next generation sequencing. Values are currently capped at 12 copies.



Copy Number Alterations

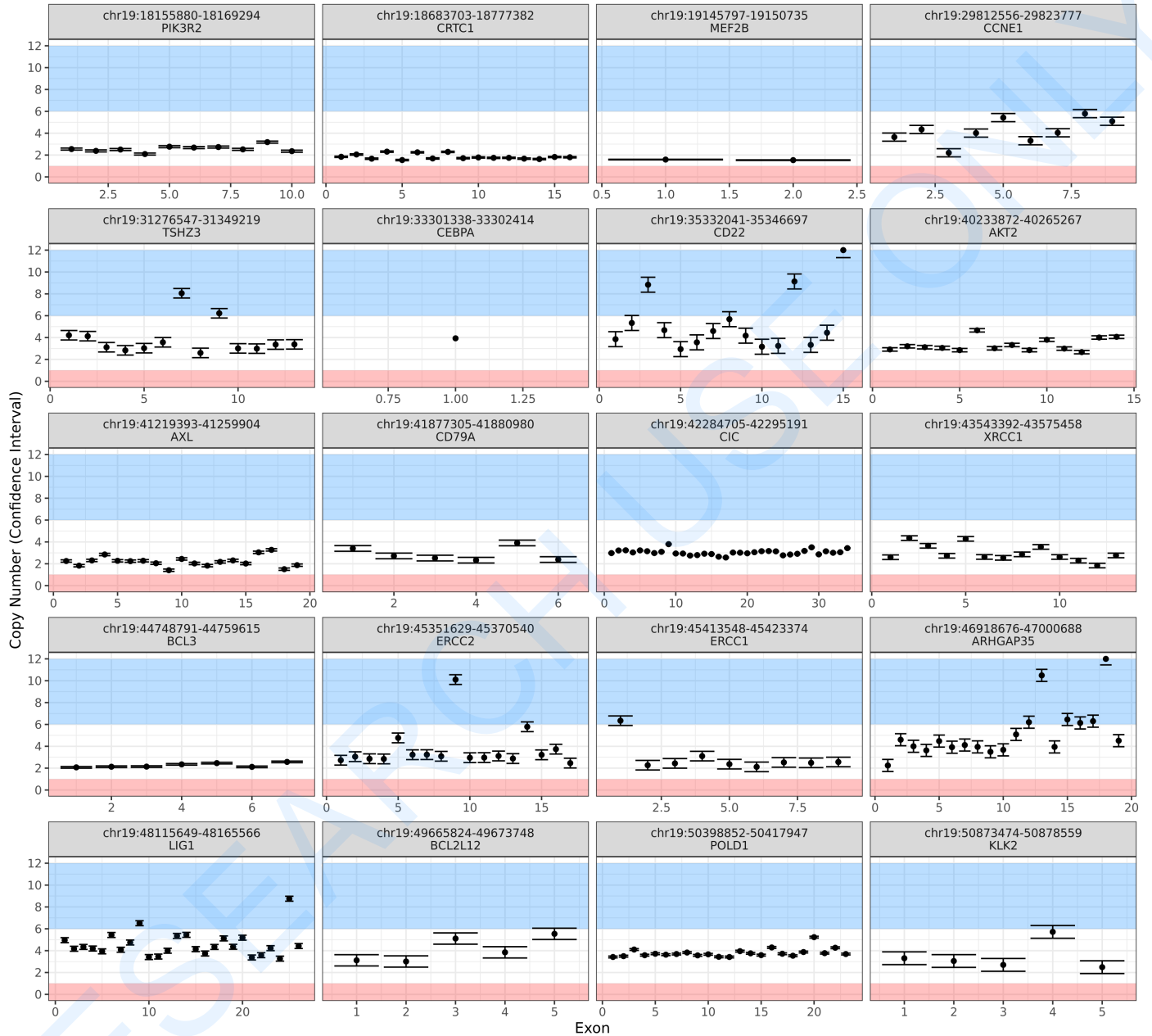


Copy number alterations by whole exome sequencing (WES):

The following plots provide estimated copy number values (black circle, y-axis) of exons per gene (x-axis), organized by chromosome (grey headers). Respective confidence intervals of each copy number call is also plotted for examining statistical error associated with next generation sequencing. Values are currently capped at 12 copies.



Copy Number Alterations

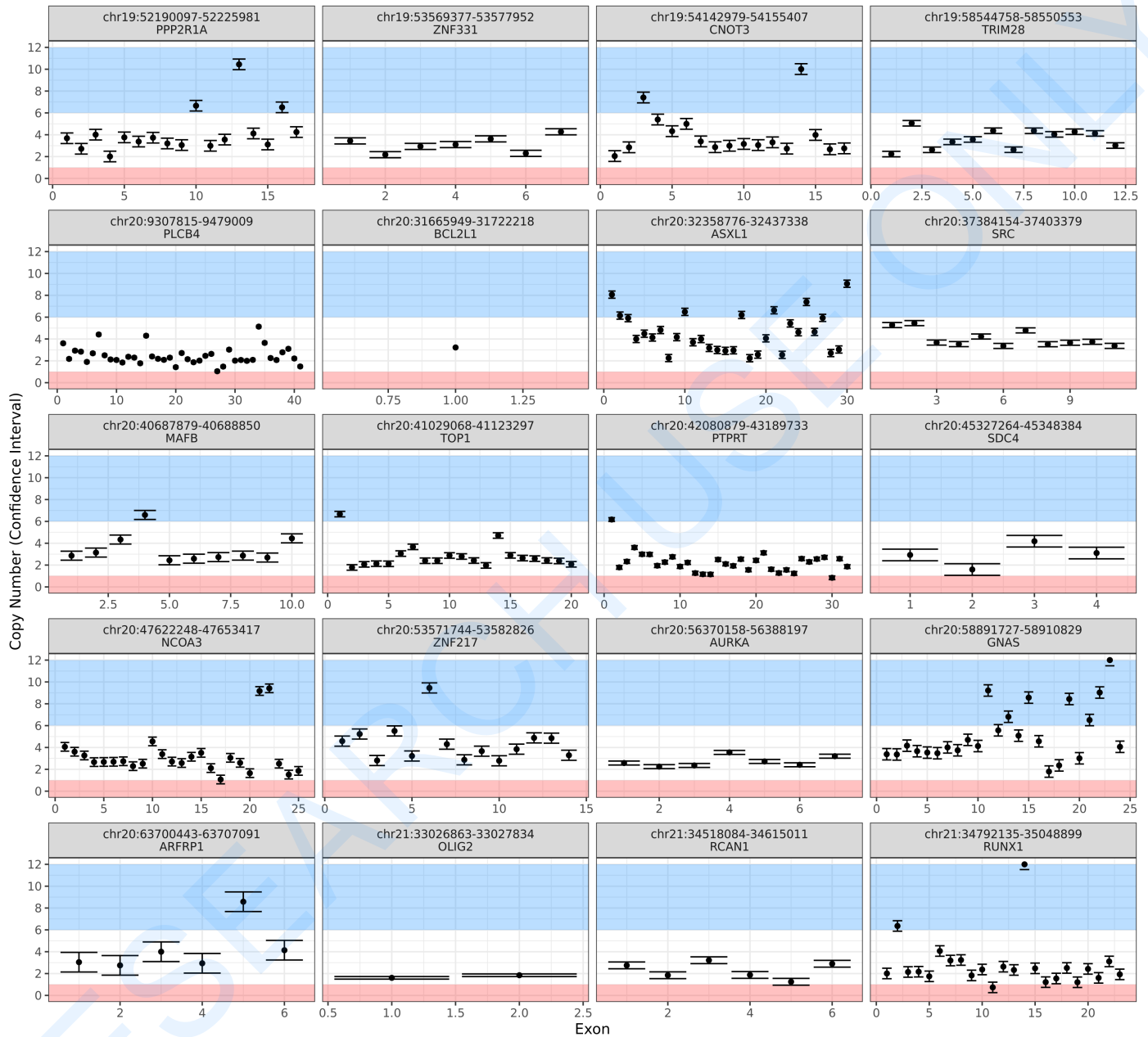


Copy number alterations by whole exome sequencing (WES):

The following plots provide estimated copy number values (black circle, y-axis) of exons per gene (x-axis), organized by chromosome (grey headers). Respective confidence intervals of each copy number call is also plotted for examining statistical error associated with next generation sequencing. Values are currently capped at 12 copies.



Copy Number Alterations

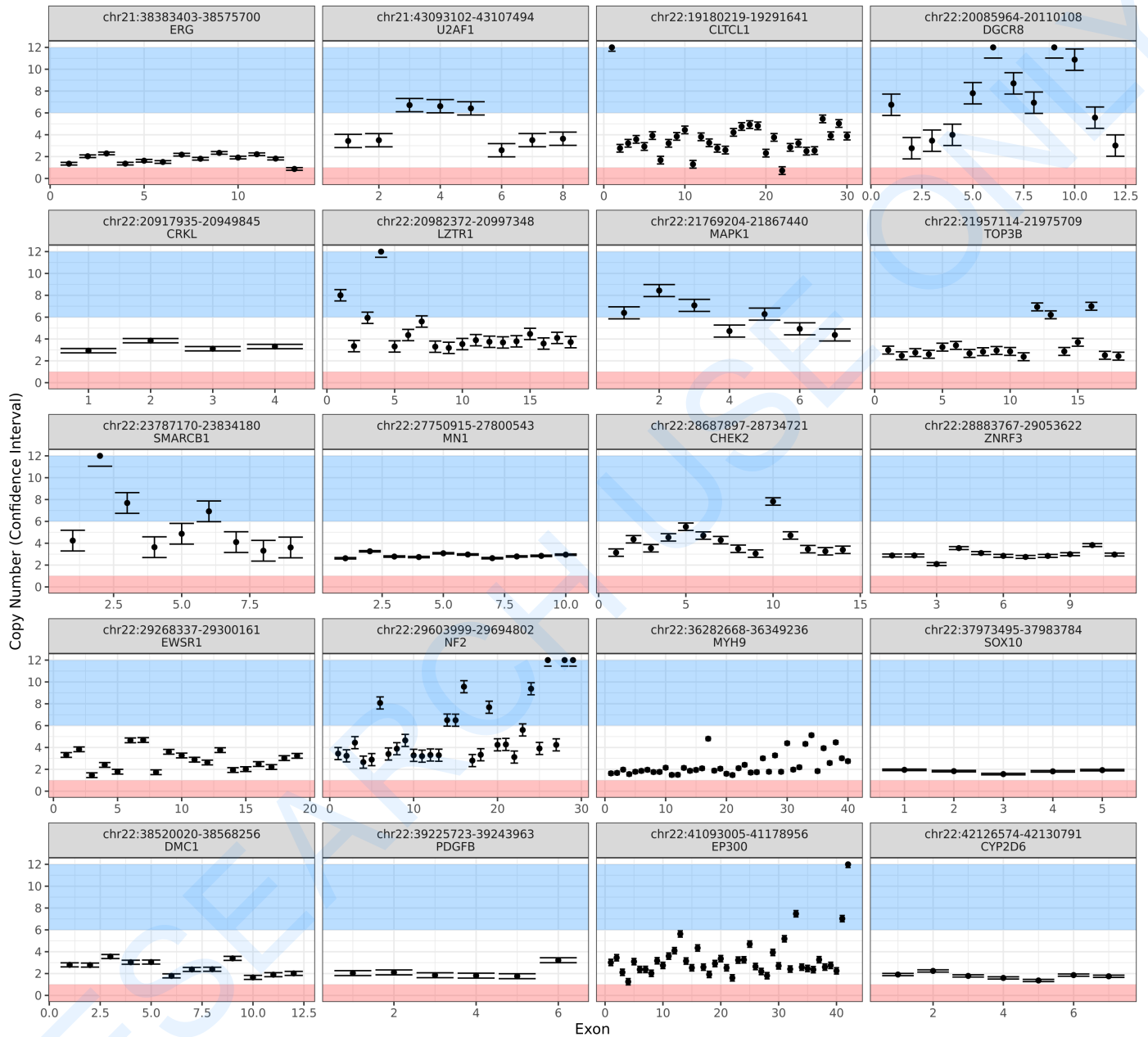


Copy number alterations by whole exome sequencing (WES):

The following plots provide estimated copy number values (black circle, y-axis) of exons per gene (x-axis), organized by chromosome (grey headers). Respective confidence intervals of each copy number call is also plotted for examining statistical error associated with next generation sequencing. Values are currently capped at 12 copies.



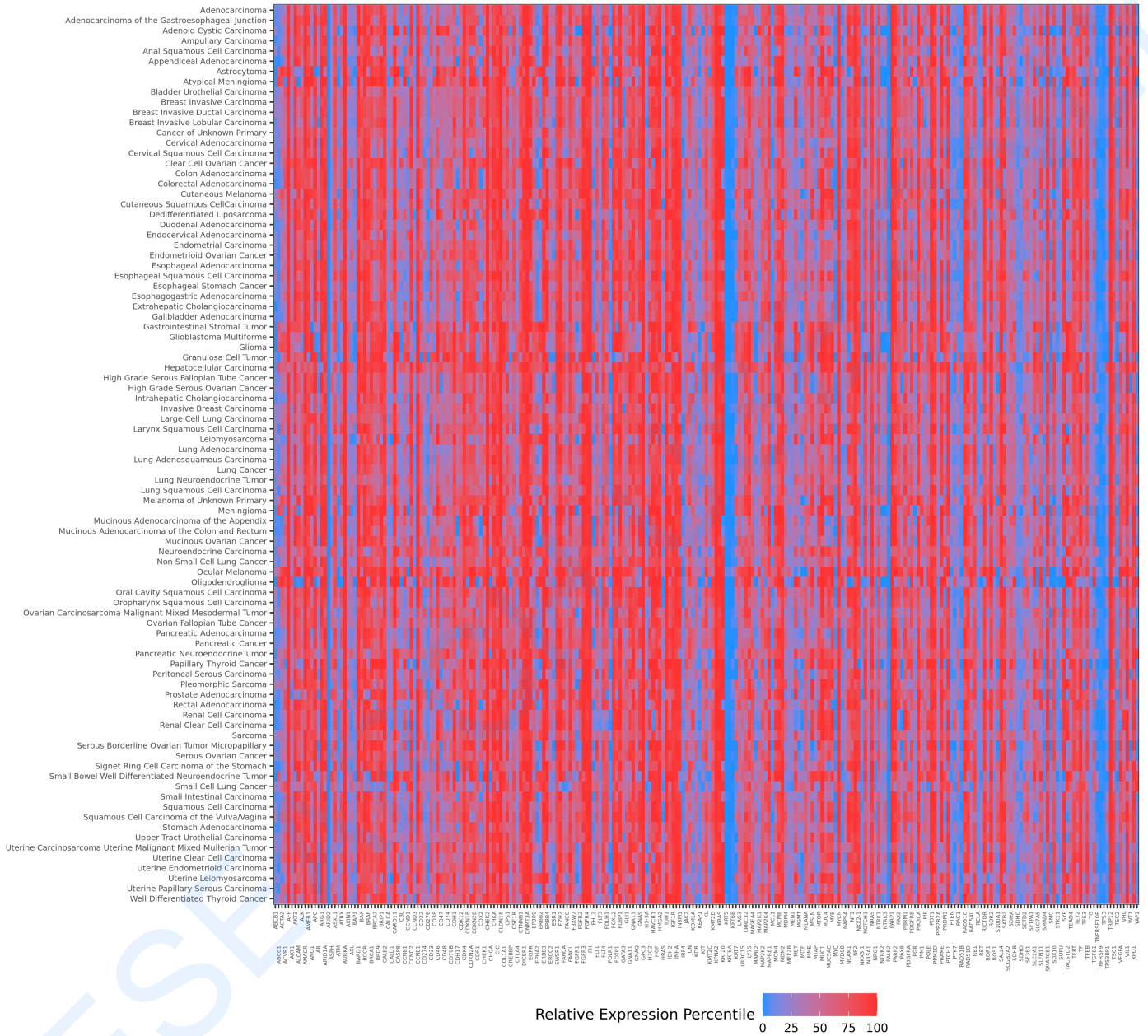
Copy Number Alterations



Copy number alterations by whole exome sequencing (WES):

The following plots provide estimated copy number values (black circle, y-axis) of exons per gene (x-axis), organized by chromosome (grey headers). Respective confidence intervals of each copy number call is also plotted for examining statistical error associated with next generation sequencing. Values are currently capped at 12 copies.

Relative RNA Expression



Gene expression is derived from whole transcriptome sequencing (WTS).

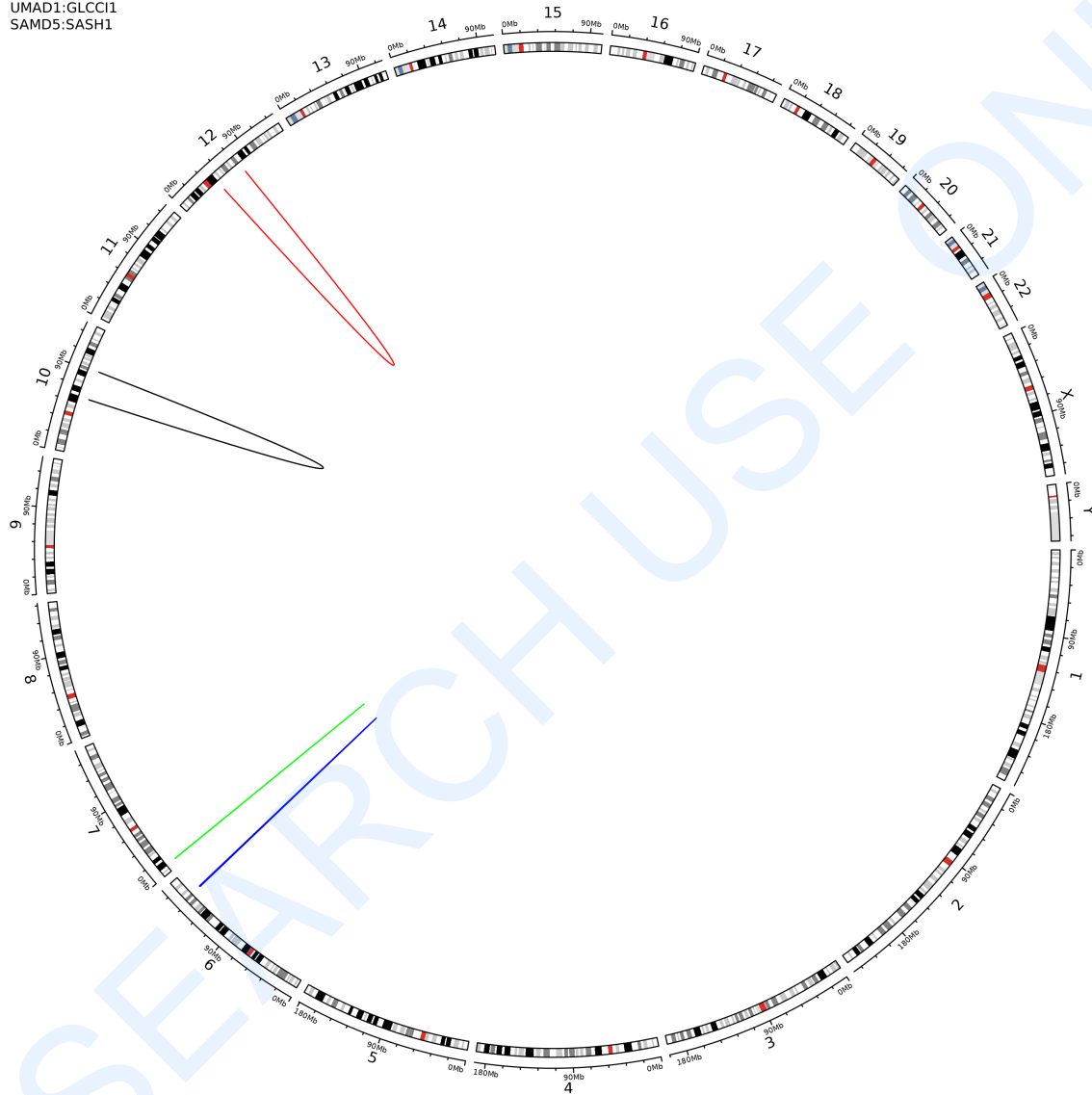
Relative expression of genes is calculated as normalized values using Transcripts per Million Molecules (TPM), for which a percentile is derived by comparison to a distribution of Caris data across multiple tumor types. The blue-red gradient represents the relative expression percentile of a specific gene (x-axis) across these different tumor types (y-axis). Darker red indicates the sample exhibits overexpression of the gene relative to all other samples analyzed within that tumor type.

TN26-



RNA Gene Fusions

- CPEB3:ANK3
- ANO6:GLIPR1L2
- UMAD1:GLCCI1
- SAMD5:SASH1



RNA Fusions via Whole Transcriptome Sequencing:

RNA read alignments are created using FPGA-adapted STAR Aligner. Fusions are detected by FPGA-adapted STAR-Fusion which is a component of the Trinity Cancer Transcriptome Analysis Toolkit (CTAT). The STAR alignment software maps junction reads and spanning reads to a reference annotation set (hg38). STAR-Fusion uses the aligned output from STAR to produce fusion calls and read statistics. STAR-Fusion performs a fast mapping of fusion evidence to reference transcript structure annotations and filters likely artifacts to report accurate fusion predictions. We have developed and optimized a new normalized reads score called nReads which takes the total fusions reads found and modifies it based on an exponential distribution that matures a classic saturation curve. This score weighs both junction and spanning reads equally and also normalizes for the total RNA mapped reads. A threshold of this score has been optimized to call fusion events with highest sensitivity, PPV, and specificity. The displayed fusions are not necessarily in-frame.

TN26-